

**Universitatea Națională de Știință și Tehnologie
POLITEHNICA București
Faculty of Biotechnical Systems Engineering**



**Universitatea Națională
de Știință și Tehnologie
POLITEHNICA BUCUREȘTI**

Summary of the Doctoral Thesis

***RESEARCH ON THE REALIZATION OF AN ELECTRICALLY
OPERATED SELF-PROPELLED AGRICULTURAL VEHICLE***

SCIENTIFIC ADVISOR:

Professor Ph.D. Eng. Sorin-Ștefan BIRIȘ

AUTHOR:

Cristea Mario

Bucharest, 2023

ABSTRACT

The value that the tractor has gained on farms has increased rapidly over time, becoming one of the farmer's main technical systems. As a result, tractor manufacturers can add additional functions to the tractor or make modifications to make them more powerful, faster, more comfortable, and with the ability to perform increasingly diverse tasks.

This thesis's overall objective is to conduct research and experiments on the dynamic and energetic behavior of a self-propelled electric agricultural vehicle. In this work, from a theoretical perspective, a mathematical model has been developed regarding the forces acting on a 4x2 or 4x4 traction tractor, the engine power required, as well as the torque needed for optimal tractor movement on different types of soil, the dynamic behavior of the tractor, and how dynamics can be influenced when the center of gravity is changed without adding additional weights to the tractor's axles. From an experimental perspective, the following aspects were considered: determining the physical parameters of the four electric agricultural vehicles, their maximum and optimal travel speeds, vehicle dynamics under real working conditions, braking distances, noise produced by each vehicle, and electricity consumption for real working situations. The data obtained in the experiments were tables, and calculations were performed using Microsoft Excel, Microsoft 365 version. Graphs were created using Microsoft Excel and the Python programming language, with specific libraries for working with large tables.

REZUMAT

Valoarea pe care tractorul a căpătat-o în cadrul fermelor a crescut foarte repede în timp ajungând să fie unul dintre sistemele tehnice principale ale fermierului. Ca urmare producătorii de tractoare reușesc să adauge funcții suplimentare tractorului sau să aducă modificări astfel încât acestea au devenit mai puternice, mai rapide, mai confortabile și cu capacități de a executa lucrări din în ce mai diversificate.

Obiectivul general al tezei îl constituie realizarea de cercetărilor și experimentărilor privind comportamentul dinamic și energetic al unui vehicul agricol autopropulsat acționat electric. În această lucrare, din punct de vedere teoretic, a fost elaborat un model matematic privind forțele care acționează asupra unui tractor cu tracțiune 4x2 sau 4x4, necesarul forței motorului cât și al cuplului pentru o deplasare în condiții optime a tractorului pe diferite tipuri de sol, comportamentul dinamic al tractorului și modul cum poate fi influențată dinamica atunci când, fără adăugarea de greutate suplimentare pe punțile tractorului, se modifică centrul de greutate. Din punct de vedere experimental s-au avut în vedere următoarele aspecte: determinarea parametrilor fizici a celor 4 vehicule agricole electrice, vitezele maxime de deplasare dar și cele optime de deplasare, dinamica vehiculelor în condiții reale de lucru, distanțelor de frânare, zgomotul produs de fiecare vehicul în parte și consumul de energie electrică pentru situații reale de lucru. Datele obținute în cadrul experimentelor au fost sub forma de tabele iar calculele au fost realizate folosind programul Microsoft Excel versiunea Microsoft 365. Pentru realizarea graficelor a fost folosit programul Microsoft Excel dar și cu ajutorul limbajului de programare Python la care au fost adăugate librării specifice lucrului cu tabele de mari dimensiuni.

ACKNOWLEDGMENTS

At the end of this stage of my life, I wish to address a few words of gratitude to all those who have been with me, guided me, and supported me throughout these years required for the completion of this doctoral thesis.

With deep respect, I extend my heartfelt thanks to Professor Sorin-Ștefan BIRIȘ, Ph.D., Eng., who, as my supervisor, guided me and provided all the support and assistance I needed throughout the entire research and thesis development period.

I express my gratitude to Univ. Prof. Ph.D. Eng. Gheorghe VOICU, Prof. Ph.D. Eng Edmond MAICAN, Prof. Ph.D. Habil. Eng Cristina Ileana Covaliu-Mierlă, and Lect. Ph.D. Eng. Mihaela Florentina DUȚU for their constant support, suggestions, and encouragement throughout the elaboration of the doctoral thesis.

Sincere thanks to my colleagues at the National Research and Development Institute for Machines and Installations for Agriculture and Food Industry (INMA) in Bucharest, particularly to Ph.D. Valentin VLĂDUȚ, Ph.D. Mihai MATAACHE, Ph.D. Iulian-Florin VOICEA, Ph.D. Stud. Gabriel GHEORGHE, Ph.D. Radu CIUPERCĂ, and Ph.D. Stud. Cătălin PERSU for their moral support, suggestions, and encouragement, as well as for providing the necessary equipment during the entire period of thesis development.

I thank all the members of the doctoral committee for their patience in reviewing the thesis and for the suggestions they made.

Finally, I extend my gratitude to all the members of my family for their understanding and support during this period.

Table of content

ABSTRACT	1
ACKNOWLEDGMENTS.....	2
FOREWORD	5
Chapter 1 The tractor in agriculture	6
Introduction	6
1.1 The Role and Importance of Tractors in Romania	6
1.2. The Necessity and Importance of Tractors in Agricultural Cultivation	6
1.3. The Physical and Mechanical Properties of Agricultural Tractors (Dimensions, Weight, Power).....	7
Chapter 2 The current state of agricultural tractors	8
2.1. The current status of agricultural tractors being manufactured worldwide.....	8
Chapter 3 The main working parameters of agricultural tractors – mathematical models	10
3.1. Dynamic parameters	10
3.2 Conversion of engine torque into propulsive force	10
3.3. Kinematics of the wheel.....	11
3.4. Wheel dynamics on rigid ground	13
3.5. The dynamics of the driven wheel on deformable terrain.....	13
3.6. Drive wheel dynamics on non-deformable ground	15
3.7. Dynamics of the drive wheel on deformable terrain	17
3.8. Wheel slippage.....	18
3.9. Center of mass and coordinates of center of gravity.....	18
3.10 The dynamics of the tractor	20
3.10.1. Dynamics of the 4x2 tractor.....	20
3.10.2. The dynamics of tractors that are equipped with 4X4 traction.....	23
3.11. Longitudinal stability	26
Chapter 4 The current state of construction of tractors and chassis intended for equipping with electric motors	29
4.1 The propulsion system of tractors equipped with internal combustion engines	29
4.1.1 The engine.....	29
4.1.2 Transmission.....	29
4.2. The components of the electric propulsion systems	30
4.2.1. Types of electric motors	30
4.2.2. Types of accumulator batteries.....	31
4.2.3. Types of motor controllers	32
4.2.4. Types of DC/DC converters.....	32
4.2.5. Types of chargers.....	33
4.2.6. Types of battery management systems (BMS)	34
Chapter 5 Experimental research on the realization of electrically driven agricultural vehicles	35
5.1. Analysis of the possibility of replacing an internal combustion engine with an electric one and studying the required equipment.....	35
5.2. Tractor chassis used for experimentation	37
5.2.1 Vegetable chassis.....	37
5.4. Devices, apparatus, and methods of setting, adjusting, and measuring used	39
5.4.1. Programming and control interfaces.....	39
5.4.2. PC software required for programming, configuration and control	39
5.4.3. The equipment used for measurements and control.....	39
5.5. Determinarea caracteristicilor fizice ale vehiculele agricole acționate electric.....	39
5.5.1. Determination of the mass of electric vehicles.....	39
5.5.2. Determining the motor shaft speed	39
5.5.3. Determination of battery charging time.....	40
5.5.4. Determining the masses of the tractors	40
5.5.5. Braking Safety Assessment	41
5.5.5. Determining the level of acoustic pressure around the tractor and at the tractor driver's ear	42

5.5.6. Determination of energy indices	43
5.5.6.1. Determining the speed of movement	43
5.5.6.2. Determining the consumption of electrical energy from the grid	43
5.5.6.3. Determination of Traction Force.....	44
5.5.6.4. Determination of Autonomy	44
5.5.6.5. Fuel Economy.....	45
Chapter 6 Theoretical Research on the Development of Electrically Powered Agricultural Vehicles ..	48
6.1. Force and Torque Required for Tractor Movement.....	48
6.1.1. Case of Travel on a Horizontal Surface.....	48
6.1.2. Case of Travel on an Inclined Surface.....	49
6.2. Calculation of the minimum torque required for tractor movement.....	49
6.3 Calculation of the required power for the propulsion system.....	51
6.4 Calculation of the center of gravity	53
6.5. Changing the position of the center of gravity.....	55
6.6. Total efficiency	61
6.7. Rotor Slip	61
6.8. Energy Consumption	62
6.9. Battery charging	64
Chapter 7 General conclusions, contributions, perspectives.....	65
7.1. Conclusions.....	65
7.2. Personal contributions.....	65
7.3. Perspectives.....	66
List of works	66
Patent application.....	67
Utility model application.....	67
Selective Bibliography.....	68
Annexes	70
Abbreviations	70
List of notations	70

FOREWORD

The Doctoral Thesis "Research on the Development of a Self-Propelled Agricultural Vehicle Driven by Electricity" has as its main objective the theoretical and experimental research on the dynamic and energetic behavior of four agricultural tractor chassis, on which an electric propulsion system powered by a battery was mounted.

The work comprises 7 chapters, 233 pages, 161 figures, 43 graphs, 43 tables, 224 mathematical relationships, 21 appendices, and 91 bibliographic references.

In Chapter 1, "The Tractor in Agriculture," the history, role, and importance of tractors in global and Romanian agriculture, the general properties of tractors, and the thesis objectives are presented.

In Chapter 2, "The Current State of Agricultural Tractors," the level of development reached by tractors worldwide and in Romania is presented, as well as the electrical components that can be installed on tractors to achieve electric propulsion, with a detailed description of their characteristics and performance.

In Chapter 3, "Main Working Parameters of Agricultural Tractors - Mathematical Models," the mathematical modeling of dynamic parameters, tractor and wheel kinematics, wheel slip phenomenon, tractor's center of mass, and the dynamics of 4X2 and 4X4 tractors are detailed.

In Chapter 4, "The Current State of Tractor and Chassis Construction for Electric Motor Installation," the components used in the construction of a conventional tractor with an internal combustion engine are presented, as well as new models of robots and electric tractors used in agriculture. Additionally, types of electric motors, batteries, motor controllers, and battery chargers used in research on using electric motors for propulsion are presented.

In Chapter 5, "Experimental Research on Electrically Driven Agricultural Vehicles," the solutions adopted to replace the internal combustion engines mounted on agricultural tractors with electric motors powered by a battery are presented, along with the methods and technical measurement systems used for programming and configuring the system, determining the physical characteristics of the agricultural vehicles used in experiments, and determining the energy indices.

In Chapter 6, "Theoretical Research on Electrically Driven Agricultural Electric Vehicles," calculations are presented for determining the minimum force that the electric motor must provide to move the system on flat or inclined surfaces at different angles, determining the minimum torque required for tractor movement, determining the consumption of electrical energy during motion and for auxiliary equipment, vehicle dynamics, and the values of electrical quantities measured during experiments.

In Chapter 7, "General Conclusions, Contributions, and Perspectives," general conclusions, contributions made by this work in the documentary, theoretical, and experimental domains, and perspectives for the use of electrical energy in the field of agricultural vehicles are presented.

Chapter 1 The tractor in agriculture

Introduction

From its inception until it became the intelligent machine we see today, the tractor has traveled a long and complex path, resulting from intricate evolutionary processes in science and technology, among other factors. The discovery and improvement of steam engines and internal combustion engines were pivotal in the tractor's development. The first steam-powered tractors appeared in England and France before the mid-19th century and were primarily used in the military and transportation industries.

The first documented mention of agricultural tool imports in the Romanian Principality dates to 1830. A few years later, the Agricultural Society was founded, and the model farm in Pantelimon was established, where steam-powered tractors were used. In 1835, Prince Ghica initiated the establishment of the "Agricultural Society," whose primary role was to popularize and experiment with agricultural machinery.

1.1 The Role and Importance of Tractors in Romania

Romania possesses a significant agricultural land area, approximately 14 million hectares, with 9.7 million hectares categorized as arable land. This places Romania in the 7th position among European countries. The modern technical cultivation of such vast expanses requires a complex technical-material base, with agricultural tractors playing a significant role.

Agricultural tractors can be considered multifunctional agricultural machinery due to their ability to use a wide range of agricultural accessories in various agricultural activities. Analyzing statistical data from the website www.madr.ro, the tractor fleet in Romania is continuously growing (see Figure 1.1).

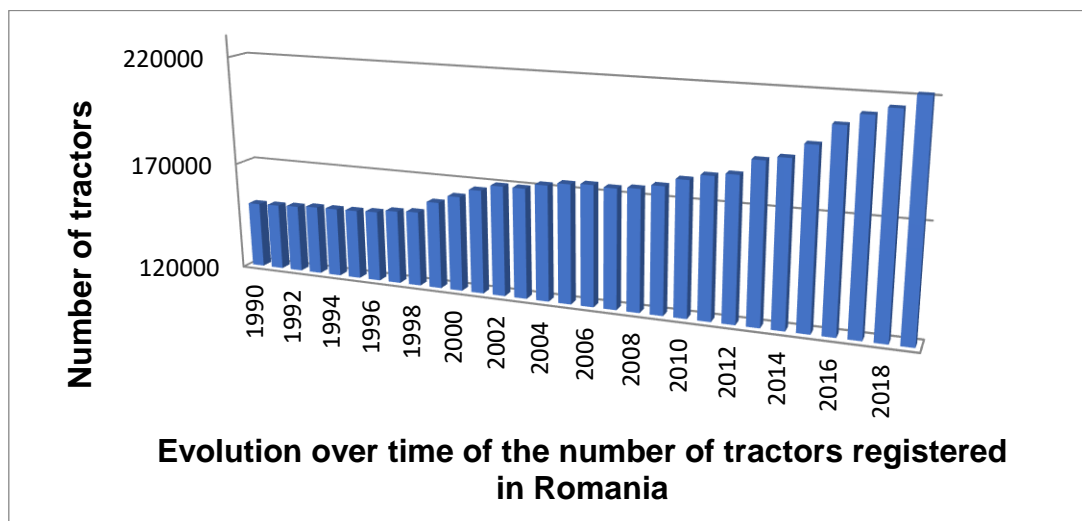


Figure 1.1 Tractor Fleet Growth in Romania

1.2. The Necessity and Importance of Tractors in Agricultural Cultivation

Modern agriculture has evolved in stages due to the industrial development that has taken place over time, primarily in the 20th century when agricultural mechanization and technological advancements began. The primary source of energy for agricultural operations is the tractor, serving as the central element in a system composed of agricultural machinery. The emergence and development of tractors in agriculture has assisted farmers in increasing agricultural production and optimizing farm operations.

1.3. The Physical and Mechanical Properties of Agricultural Tractors (Dimensions, Weight, Power)

Modern agricultural tractors must adhere to regulations and standards concerning safety, environmental protection, and the requirements for use in agricultural operations. An example of such regulations that impose norms for agricultural tractors is Regulation No. 167/2013 of the European Parliament and the Council, dated February 5, 2013. [2]

Table 1.1 presents the classification of tractors based on the criteria of traction class.

Table 1.1 Classification of tractors according to the traction class criterion

Traction class	1	2	3	4	5	6	7	8	9	10	11	12	13	14
Traction force (KN)	2	6	8	14	20	30	40	50	60	80	100	150	250	350

For agricultural tractors, the rated drawbar pull is the force at which a tractor - working in a field with normal compaction and moisture - achieves maximum traction efficiency with an allowable wheel slip of 8-12% for 4x4 wheel tractors, 10-15% for 4x2 wheel tractors, and 5% for tracked tractors.

Chapter 2 The current state of agricultural tractors

2.1. The current status of agricultural tractors being manufactured worldwide

Fuels used in agriculture are generally fossil fuels or biofuels. The most common fuels are gasoline and diesel. The most frequently used biofuels in agriculture include vegetable oil, biodiesel, biogas, bioethanol, and biomethanol.

Global concerns about reducing environmental pollution have led to the development of procedures and the creation of anti-pollution equipment in industry. Accredited organizations have established new standards for pollution from both industry and transportation each year. Car manufacturers have begun developing and producing vehicles that are powered by less polluting engines or even have zero emissions.

As a result, pollution standards like Euro 1, Euro 2, and up to Euro 6 have been introduced. Additionally, hybrid propulsion systems, hydrogen-powered engines, and battery-powered vehicles have been developed. Many tractor and agricultural equipment manufacturers are researching or have already produced equipment powered by electric motors. The reasons for intensifying research in this direction are manifold, ranging from reducing pollution to optimizing processes through the implementation of artificial intelligence.

Manufacturers are preparing for future models of agricultural vehicles that have the capability to be environmentally friendly by introducing propulsion and auxiliary systems powered by battery accumulators, as exemplified by the Fendt tractor shown in Figure 2.1.



Figure 2.1 Fendt e100 Vario electric tractor [6]

John Deere has made significant advancements. They have already developed electric tractors of various power levels designed for both large and small farms. These tractors are equipped with remote control systems but can also operate autonomously. They are integrated into communication networks and can transmit data both amongst themselves and to a control center. These tractors are equipped with artificial intelligence. This enables many agricultural tasks to be carried out with minimal losses and in a reduced timeframe.

The autonomous electric prototype tractor produced by John Deere can be equipped with wheels or tracks and features a 500 kW electric motor. It was first showcased at Agritechnica Germany in 2019 (Figure 2.2) [9]



Figure 2.2 John Deere autonomous electric tractor [9]

The manufacturer Rigitrac also has an electric tractor prototype, the SKE-50 (Figure 2.3), developed in collaboration with the University of Applied Sciences in Buchs, Switzerland. The tractor is equipped with four electric motors, one for each axle, with the other two used for power take-offs at the front and rear. The total power of the vehicle is 50 kW. [13]



Figure 2.3 Tractor SKE-50 produced by Rigitrac [13]

Chapter 3 The main working parameters of agricultural tractors – mathematical models

3.1. Dynamic parameters

The dynamic performance of the tractor is influenced by the dynamic performance of the engine. Therefore, by knowing the characteristics of the engine, the most important tractor operating parameters can be deduced.

The dynamic factor is defined by the following equation:

$$D = \frac{F_m - F_a}{G_a} \quad (3.1)$$

Resistance forces vary over a very wide range depending on the working environment. Ideally, a tractor's engine should deliver constant power regardless of the operating regime. In this case:

$$P_m = M \omega = ct. \text{ sau } M n = ct. \quad (3.2)$$

The rated power and rated torque, denoted as P_n and M_n , occur at the engine's rated speed. For internal combustion engines, the following idle speed calculation relationship is used:

$$n_g = (1,06 \dots 1,15) n_n \quad (3.3)$$

In internal combustion engines, there are differences even between the two types of engines commonly used in tractors, namely: spark-ignition engines (gasoline engines) which, if operated for an extended period at the rated speed, tend to overheat. This results in the engine operating outside its parameters, potentially causing operational anomalies.

For diesel engines, it has been observed that:

$$n \in (n_{min}, n_M), \frac{dM_e}{dn} > 0 \quad (3.4)$$

resulting in unstable operation.

While for:

$$n \in (n_m, n_g), \frac{dM_e}{dn} < 0 \quad (3.5)$$

the engine operates steadily.

Engines can be categorized as highly adaptable or elastic. The adaptability coefficient is defined as:

$$K_a = \frac{M_{max}}{M_n} \quad (3.6)$$

The elasticity coefficient is defined by the following equation:

$$c = \frac{n_n}{n_M} = \frac{\omega_n}{\omega_M} \quad (3.7)$$

The kinetic energy required to move the tractor is described by the following relationship:

$$E = \frac{1}{2} J_{mm} (\omega_n^2 - \omega_M^2) = \frac{1}{2} J_{mm} \omega_n \left(1 - \frac{1}{c^2}\right) \quad (3.8)$$

In conclusion, the greater the "c," the higher the engine's capacity to facilitate tractor movement. It can be said that an internal combustion engine is more elastic when "c" is higher, and the two coefficients, k, have values: $k = 1.20 - 1.35$, $c = 1.5 - 2.25$ for gasoline engines, and $k = 1.05 - 1.20$, $c = 1.25 - 1.55$ for diesel engines.

3.2 Conversion of engine torque into propulsive force

The torque generated by the engine is transmitted to the wheels through the transmission. However, of all the subassemblies that make up the transmission, only a portion

is used for the actual transmission of torque from the engine. The total transmission ratio is the product of the ratios of all the subassemblies that make up the transmission and is:

$$i_{tr} = i_{tmc} i_{cv} i_{tc} i_{tf} \quad (3.9)$$

The transmission of torque from the engine to the wheels occurs with losses. These losses take place throughout the transmission chain and can be highlighted in the transmission efficiency, which can be simplified using the expression:

$$\eta_{tr} = \frac{P_m}{P_e} = \frac{M_m}{M_e i_{tr}} \quad (3.10)$$

The total efficiency can also be calculated using the expression:

$$\eta = \eta_{tmc} \eta_{cv} \eta_{card} \eta_{tc} \eta_{tf} \quad (3.11)$$

Transmission efficiencies can be determined experimentally through measurements of the moments that occur in the transmission shafts and the engine shaft. However, in general, these efficiencies are known and organized in calculation tables. For example, for tractors, the efficiency ranges from 0.86 to 0.89.

In the above relationships, moments can be replaced with forces acting at a distance from a reference point, typically an axis.

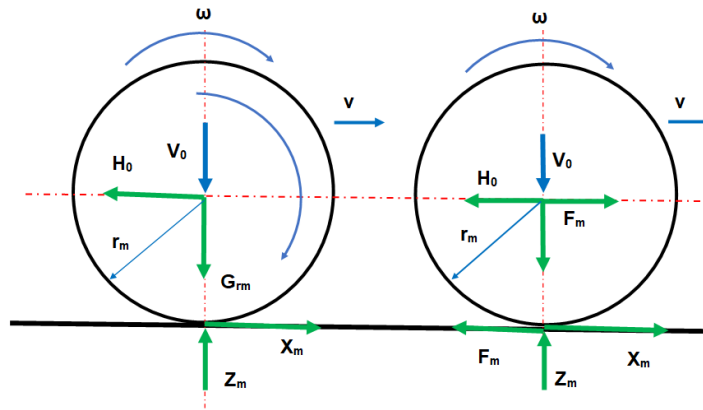


Figure 3.1 The forces and moments acting on the drive wheel [35]

$$F_m = \frac{M_{mr}}{r_m} = \frac{M_e i_{tr} \eta_{tr}}{r_m} \quad (3.12)$$

The maximum engine torque determines the maximum value of the force "F_m":

$$F_m = \frac{M_m}{r_m} = \frac{M_e i_{tr} \eta_{tr}}{r_m} \quad (3.13)$$

Displacement occurs when the actual driving force is greater than or equal to the force determined by the resistances opposing the movement.

3.3. Kinematics of the wheel

The wheel's movement during travel is considered in a parallel plane. However, in ideal conditions, the terrain is considered non-deformable and flat, and the wheel does not deform under the influence of loads that occur during movement. From Euler's equation, the distribution of velocities is derived as follows:

$$\vec{V} = \vec{V}_r + \vec{\omega}_i \vec{r} \quad (3.14)$$

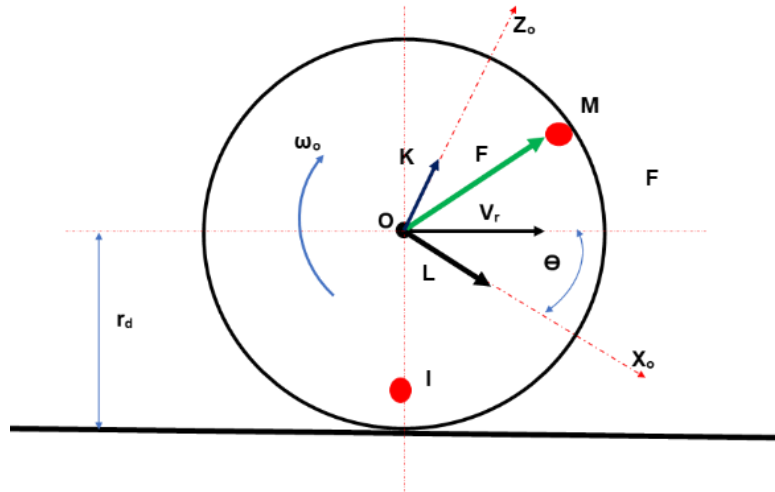


Figure 3.2 The position of the wheel's center of rotation

The mobile reference system is $OX_oY_oZ_o$ (Figure 3.2), and the relationships defining the vectors are as follows:

$$\vec{V}_r = v_r \cos \theta \bar{i} + v_r \sin \theta \bar{k} \quad (3.15)$$

$$\vec{\omega} = \vec{\omega}_j \quad (3.16)$$

$$\vec{r} = x \bar{i} + z \bar{k} \quad (3.17)$$

This results in Equation (3.14) becoming;

$$v = v_r \cos \theta \bar{i} + v_r \sin \theta \bar{k} + \begin{bmatrix} \bar{i} & \bar{j} & \bar{k} \\ 0 & \omega & 0 \\ x & 0 & z \end{bmatrix} \quad (3.18)$$

$$v_x = v_r \cos \theta + \omega z \quad (3.19)$$

$$v_y = 0 \quad (3.20)$$

$$v_z = v_r \sin \theta - \omega x \quad (3.21)$$

The coordinates of the point "I", which is in the xoy plane and has zero velocity at a certain moment, are:

$$x_I = \frac{v_r}{\omega} \sin \theta \quad (3.22)$$

$$z_I = \frac{v_r}{\omega} \cos \theta \quad (3.23)$$

Depending on the variation of the ratio v_r/ω and the radius from the wheel center to the ground, the following cases are distinguished:

1. $OI = \frac{v_r}{\omega} = r_d$ in which case the actual velocity is equal to the theoretical velocity;

The actual velocity is equal to the theoretical velocity.

2. $OI = \frac{v_r}{\omega} < r_d$ in which case the actual velocity is less than the theoretical velocity, and slipping occurs;

$$\sigma = \frac{v_{pat}}{v_t} = \frac{v_t - v_r}{v_t} = \frac{\Delta r_d}{r_d} \quad (3.24)$$

$$v_r = v_t(1 - \sigma) \quad (3.25)$$

3. $OI = \frac{v_r}{\omega} > r_d$ in which case the actual velocity is greater than the theoretical velocity, and sliding occurs;

$$\varepsilon = \frac{v_r - v_t}{v_t} = \frac{v_{al}}{v_t} = \frac{\Delta r_d}{r_d} \quad (3.26)$$

$$v_r = v_t(1 + \varepsilon) \quad (3.27)$$

The occurrence of slipping is specific to driving wheels, while sliding occurs on the driven wheels.

3.4. Wheel dynamics on rigid ground

When the tire deforms, and the terrain also deforms, it represents a real working condition of the tractor.

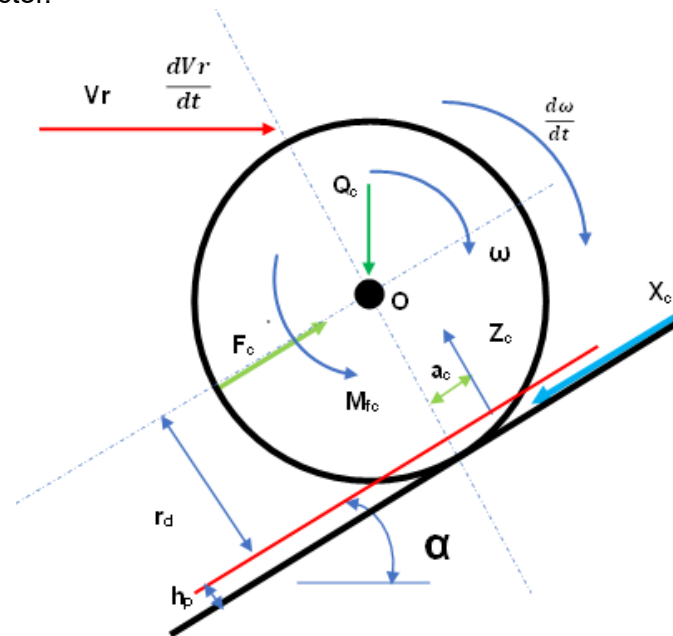


Figure 3.3 Wheel dynamics on non-deformable terrain [35]

In Figure 3.3, we have the forces and moments governing the dynamics of the wheel on rigid terrain.

The equations of motion are as follows:

$$m_c \frac{dv_r}{dt} = F_c - Q_c \sin \alpha - X_c \quad (3.28)$$

$$Q_c \cos \alpha - Z_c = 0 \quad (3.29)$$

$$J_c \frac{d\omega}{dt} = X_c r_d - Z_c a_c - M_{fc} \quad (3.30)$$

After substitutions and manipulation of the relationships, we obtain:

$$F_c = Q_c \cos \alpha \frac{a_c}{r_c} + Q_c \sin \alpha + \frac{M_{fc}}{dt} r_d + \left(m_c \frac{dv_r}{dt} + J_c \frac{d\omega}{dt} \frac{1}{r_d} \right) \quad (3.31)$$

$$f_c = \frac{a_c}{r_d} \quad (3.32)$$

If we multiply the equation (3.31) by the actual speed, we obtain the power balance of the driven wheel ($F_c v_r$):

$$F_c v_r = Q_c \cos \alpha f_c v_r + Q_c \sin \alpha v_r + \frac{M_{fc}}{r_d} v_r + \left(m_c \frac{dv_r}{dt} + I_c \frac{d\omega}{dt} \frac{1}{r_d} \right) v_r \quad (3.33)$$

Where: $F_c v_r$ is the power received by the wheel from the chassis; $Q_c \cos \alpha f_c v_r$ is the power needed to overcome rolling resistance; $Q_c \sin \alpha v_r$ is the power required for uphill climbing; $\frac{M_{fc}}{r_d} v_r$ is the power needed to overcome bearing friction; $\left(m_c \frac{dv_r}{dt} + I_c \frac{d\omega}{dt} \frac{1}{r_d} \right) v_r$ is the power required for wheel acceleration;

When tire deformation occurs, the hysteresis phenomenon takes place due to the internal friction within the tire.

3.5. The dynamics of the driven wheel on deformable terrain

In this case, the forces and moments that occur at the wheels when the terrain is deformable are explained. Since the forces and moments acting on the wheel are identical to those that occur in the case of rigid terrain, only the implications resulting from the deformation of the terrain will be highlighted in the force and power balance.

Imposed conditions:

$$\alpha \text{ is equal to zero} \quad (3.34)$$

$$\frac{dv_r}{dt} = 0 \quad (3.34)$$

$$\frac{d\omega}{dt} = 0 \quad (3.34)$$

$$M_{fc} = 0 \quad (3.34)$$

As a result, the relationship between forces can be written as:

$$F_c = X_c = Q_c * f_c \quad (3.35)$$

As for powers, we have:

$$F_c * v_r = Q_c f_c v_t + Q_c f_c v_{al} \quad (3.36)$$

The power lost due to tire and terrain deformation is $Q_c f_c v_t$, and $Q_c f_c v_{al}$ is the power lost due to slippage.

$$Q_c f_c v_t = P_{hist.pneu} + P_{def.teren} \quad (3.37)$$

If the relationships 3.35 and 3.36 are introduced into the above relationship, we have the following relationships:

$$X_c v_r = P_{hist.pneu} + P_{def.teren} + X_c v_{al} \quad (3.38)$$

It follows:

$$X_c = \frac{P_{hist.pneu} + P_{def.teren}}{v_r - v_{al}} = \frac{v_r}{v_r - v_{al}} \left(\frac{P_{hist.pneu}}{v_r} + \frac{P_{def.teren}}{v_r} \right) = \frac{v_r}{v_t} \left(\frac{P_{hist.pneu}}{v_r} + X_{def.teren} \right) = (1 + \varepsilon) \left(\frac{P_{hist.pneu}}{v_r} + X_{def.teren} \right) \quad (3.39)$$

$$X_{def.teren} = \frac{P_{def.teren}}{v_r} \quad (3.40)$$

After substitution, the following relationship is obtained:

$$f_c = \frac{X_c}{Q_c} = (1 + \varepsilon) \left(\frac{P_{hist.pneu}}{v_r} + X_{def.teren} \right) \frac{1}{Q_c} \quad (3.41)$$

According to the relationship from above, it is observed that the value of f_c for situations where the wheels move on deformable terrain depends on the value of power dissipated through hysteresis and K , where K is proportional to the vertical deformation of the terrain.

$$X_{def.teren} = k \left(\frac{\sigma}{\frac{k_c}{b} + k_\gamma} \right)^{\frac{1}{n}} \quad (3.42)$$

It is noted that the value of the rolling resistance coefficient (f_c) on deformable terrain depends on $P_{hist.pneu}$ and $X_{def.teren}$, which have opposite variations.

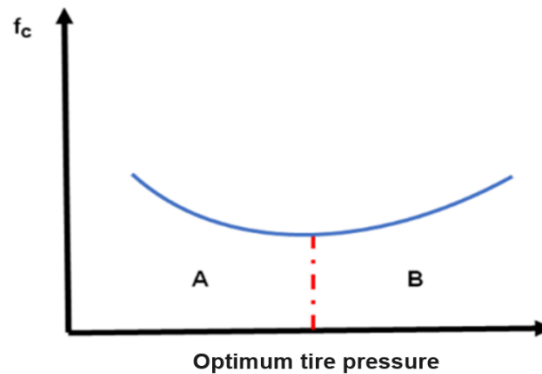


Figure 3.4 The mode of variation of the coefficient of rolling resistance

The variation of the rolling resistance coefficient can be represented by a curve that features a minimum point dividing the area under the curve into two surfaces, **A** and **B** (Figure 3.4).

There are two distinct situations in which a tire's behavior can vary depending on the internal pressure.

The first situation occurs when the tire deformation is significant, marked as "**A**". In this scenario, the friction coefficient " f_c " changes inversely proportional to the tire's internal pressure.

The second situation arises when the terrain is highly deformable, labeled as "**B**". In this context, the friction coefficient " f_c " changes directly proportional to the tire's internal pressure.

In conclusion, when moving on deformable terrain, for each type of tire, there is only one pressure value at which the rolling resistance coefficient is minimized.

3.6. Drive wheel dynamics on non-deformable ground

The situation in which movement takes place on non-deformable but sloping terrain results in a complex system of forces and moments, as explained in Figure 3.5.

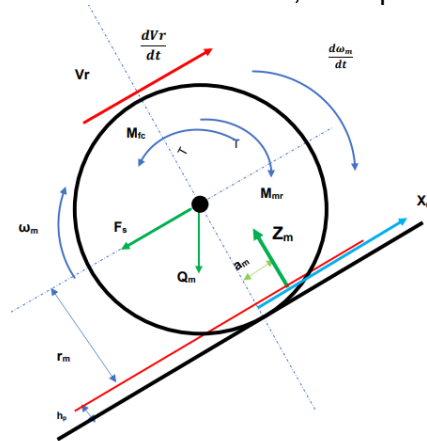


Figure 3.5 Wheel dynamics on rigid sloping ground [35]

The forces and moments that occur in the dynamics of the wheel are represented in Figure 3.5.

The dynamic radius of the wheel is:

$$r_m = r_o - h_p \quad (3.43)$$

D_a inversely depends on the tire pressure and the type of tire. The equations for motion of the wheel are:

$$m_m \frac{dv_r}{dt} = X_m - F_S - Q_m \sin \alpha \quad (3.44)$$

$$0 = Q_m \cos \alpha - Z_m \quad (3.45)$$

$$J_m \frac{d\omega_m}{dt} = M_{mr} - X_m r_m - Z_m a_m - M_{fm} \quad (3.46)$$

Using the relations from above, we can write the traction force balance on the wheel:

$$F_m = \frac{M_{mr}}{r_m} = F_S + Q_m \sin \alpha + Q_m \cos \alpha \frac{a_m}{r_m} + m_m * \frac{dv_r}{dt} + J_m \frac{d\omega_m}{dt} \frac{1}{r_m} + \frac{M_{fm}}{r_m} \quad (3.47)$$

From this relationship, it can be observed where the force generated by the engine is transmitted, specifically to the chassis movement, overcoming resistance forces, and wheel acceleration.

The simplified relationship can be written as follows:

$$F_m = \varphi_a Z_m \quad (3.48)$$

The coefficient of adhesion depends on the type of terrain, tire model, and weather conditions. The coefficient of utilization of adhesion, φ_m , is defined as– φ_m :

$$\varphi_m = \frac{F_m}{Z_m} \quad (3.49)$$

To ensure tractor movement the following condition must be met:

$$\varphi_m \leq \varphi_a \quad (3.50)$$

If friction forces are not considered and the tractor moves at a constant speed, then:

$$F_m = F_S + Z_m f_m \quad (3.51)$$

If the utilization of adhesion coefficient is added to the above relationship, the relationship becomes:

$$\varphi_m Z_m = F_S + Z_m f_m \quad (3.52)$$

$$F_S = Z_m (\varphi_u - f_m) = G_S (\varphi_u - f_m) \quad (3.53)$$

When the wheel's angular velocity is introduced into the relationship, the engine power can be written as follows:

$$P_m = M_m \omega_m = F_m r_m \omega_m = F_m v_t = F_m (v_r + v_{pat}) = F_m v_r + F_m v_{pat} \quad (3.54)$$

If the expression is detailed, it takes the following form:

$$P_m = F_S v_r + Q_m \sin \alpha v_r + Q_m \cos \alpha f_m v_r + \left(m_m \frac{dv_r}{dt} + J_m \frac{d\omega_m}{dt} \frac{1}{r_m} \right) v_r + \frac{M_{fm}}{r_m} v_r + F_m v_{pat} \quad (3.55)$$

From this relationship, it can be observed where the power generated by the engine is used. Part of it is used for the tractor's movement, overcoming slopes, wheel acceleration, overcoming all resistance, and friction, and part of the power is lost through slippage.

In this relationship, we have the following forces:

- The force reaching the wheel's axle, $F_c v_r$;
- The force required to overcome rolling resistance, $Q_m \cos \alpha f_m v_r$;
- The force required to climb a slope, $Q_m \sin \alpha v_r$;
- The force required to overcome bearing friction, $\frac{M_{fm}}{r_m} v_r$;
- The force required for wheel acceleration, $\left(m_m \frac{dv_r}{dt} + J_m \frac{d\omega_m}{dt} \frac{1}{r_m} \right) v_r$.

Replacing the relationship 3.24 results in the relationship 3.58, from which we have the power lost through slippage:

$$P_{pat} = F_m v_{pat} = F_m v_t \delta = P_m \delta \quad (3.56)$$

Thus, we can define the efficiency of the driving wheel as the sum of the useful powers depending on the power reaching the wheel:

$$\eta_{rm} = \frac{P_u}{P_c} = \frac{F_S v_r + Q_m \sin \alpha v_r + \left(m_m \frac{dv_r}{dt} + J_m \frac{d\omega_m}{dt} \frac{1}{r_m} \right) v_r}{P_r} \quad (3.57)$$

Resulting in:

$$\eta_{rm} = (1 - \delta) \left(1 - \frac{f_m}{\varphi_m} \right) = \eta_\delta \eta_f \quad (3.58)$$

$$\eta_\delta = 1 - \delta \quad (3.59)$$

$$\eta_f = 1 - \frac{f_m}{\varphi_a} \quad (3.60)$$

It follows that the efficiency of the driving wheel depends on slippage and the wheel's ground adhesion. The lower the slippage and the higher the adhesion, the higher the efficiency of the driving wheel.

3.7. Dynamics of the drive wheel on deformable terrain

The equations of motion are identical to those of the drive wheel dynamics on rigid terrain and the power balance. A constant velocity and no bearing friction are assumed.

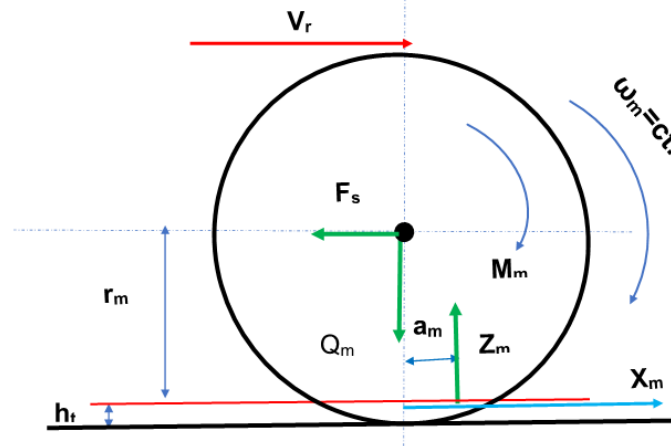


Figure 3.6 Dynamics of the drive wheel on deformable terrain [35]

The motor force:

$$F_m = F_s + Z_m f_m \quad (3.61)$$

When considering the interaction between the wheel and the terrain, we have the motor force in the following form:

$$F_m = \tau A \quad (3.62)$$

The coefficient of adhesion utilization is:

$$\varphi_m = \frac{F_m}{Z_m} = \frac{F_m}{\tau * A} = \left(\frac{A}{\tau} + tg \varphi \right) \left(1 - e^{-\frac{j}{k\delta}} \right) \quad (3.63)$$

When a wheel rotates through an angle equal to the angle at the center between two edges, the theoretically traveled distance by the wheel's axis will be: $s_t = t$ and the actual distance is $s_t = t - j$, this results in the theoretical velocity and actual velocity as:

$$v_t = \frac{t}{\Delta t} \quad (3.64)$$

$$v_r = \frac{t-j}{\Delta t} \quad (3.65)$$

The coefficient of skid is introduced into the relationship above, and we obtain:

$$\varphi_m = \varphi_{max} \left(1 - e^{-k\delta} \right) \quad (3.66)$$

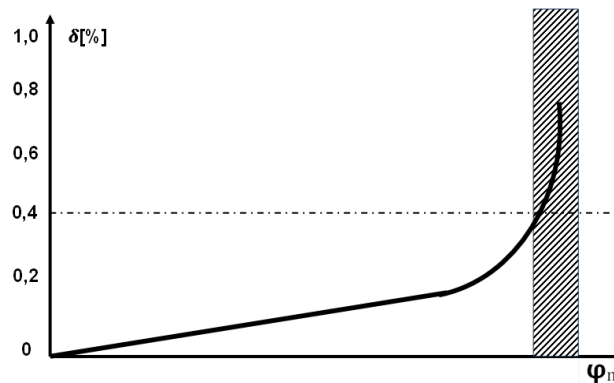


Figure 3.7 The variation of the drive wheel slip as a function of the adhesion utilization coefficient [35]

It is recommended that in calculations φ should have a value ranging between 0.6 and 0.8, and k should be between 7.5 and 25; smaller values correspond to softer terrains.

Example of calculation of slippage:

$$\delta = \frac{0,246 \varphi_m}{1 - 3,06 \varphi_m^3} \quad (3.67)$$

To simplify calculations, relative quantities are used, such as the coefficient of rolling resistance. It has the following calculation relationship:

$$f_c = \frac{D}{r_d} \quad (3.68)$$

Slippage is greatly influenced by the size of the wheels than the value of the normal stress, σ , but also the tire pressure. According to the experiments [35], it was found that the pressure in the tires must be located between relatively low limits.

3.8. Wheel slippage

When the tire is deformed, there is a mechanical thing that results in heat release. In reality, the phenomenon of wheel slippage also occurs, which is defined by the slip coefficient, δ .

This is how the coefficient of slip is defined:

$$\delta = \frac{v_{pat}}{v_t} = \frac{v_t - v_r}{v_t} = \frac{\Delta r_d}{r_d} \quad (3.69)$$

From this relationship the actual speed can be deduced:

$$v_r = v_t(1 - \delta) \quad (3.70)$$

After the mechanical work that occurs when the wheel is deformed is also introduced in relation 3.42, the following relation of the force that is required for the tractor's movement can be written:

$$Q_c \cos \alpha f_c v_r = Q_c \cos \alpha f_c (v_t - v_{pat}) = Q_c \cos \alpha f_c v_t + Q_c \cos \alpha f_c v_{pat} \quad (3.71)$$

After studying the forces that appear at the level of the wheels, it can be concluded that the movement of the tractor is dependent on the grip but also on the engine torque that is transmitted to the wheels.

So, the force that practically makes the vehicle move depends on the adhesion utilization coefficient, the rolling resistance coefficient and the normal reaction (vertical load – Q_c).

Power required for displacement is:

$$P_m = M_m \omega_m = F_m r_m \omega_m = F_m v_t = F_m (v_r + v_{pat}) = F_m v_r + F_m v_{pat} \quad (3.72)$$

3.9. Center of mass and coordinates of center of gravity

For vehicles, the center of mass or center of gravity is considered to be located in the vertical plane passing through the longitudinal axis, and it is defined by the height above the ground and the relative distance from the front and rear axles of the vehicle.

Table 3.1 Average Values for Center of Mass Parameters

Parameter	Status	Tractor unit
a/L	Empty/Loaded	0,61 - 0,67
h _g /L	Empty/Loaded	0,31 – 0,4

The calculation of the center of gravity can be determined using the centers of mass of the components that make up the tractor. The following expression is used [36]:

$$a = \frac{\sum m_i a_i}{\sum m_i} = \frac{\sum m_i a_i}{m_a} \quad (3.73)$$

$$b = L - a \quad (3.74)$$

$$h_g = \frac{\sum m_i h_i}{\sum m_e} = \frac{\sum m_i h_i}{m_a} \quad (3.75)$$

For ease of calculation, recommended average values of the equipment masses mounted on tractors have been defined in the specialized literature. An example with such data is presented in Table 3.2, where m represents the mass of the tractor. [36]

Table 3.2 Mass Values of Subassemblies Relative to Vehicle Mass

Equipment name	m_e/m [%]
Motor equipped with clutch and gearbox	12,6 – 16,0
Clutch	0,3 - 0,7
Gearbox	2,5 – 5,0
Cardan transmission	1,0 – 1,4
Rear axle	11,0 – 16,0
Front axle	1,5 – 3,5
Front suspension	1,5 – 3,5
Rear suspension	5,5 – 8,0
Wheels	17,0 – 20,0
Frame	10,0 – 15,0
Platform	11,0 – 16,0
Cabin	5,0 – 14,0

When using the values in table 3.2 the relations by which the position of the center of gravity is calculated can be written as:

$$a = \frac{\sum \frac{m_i}{m_0} a_i}{\frac{m}{m_a}} m_0 = \frac{\eta_G}{1+\eta_G} \sum \frac{m_i}{m_0} a_i \quad (3.76)$$

$$\eta_G = \frac{m}{m_u} \quad (3.77)$$

$$h_g = \frac{\sum \frac{m_i}{m_0} h_i}{\frac{m}{m_a}} m_0 = \frac{\eta_G}{1+\eta_G} \sum \frac{m_i}{m_0} h_i \quad (3.78)$$

The mass of the tractor is transmitted to the ground by means of the axles as shown in the figure below:

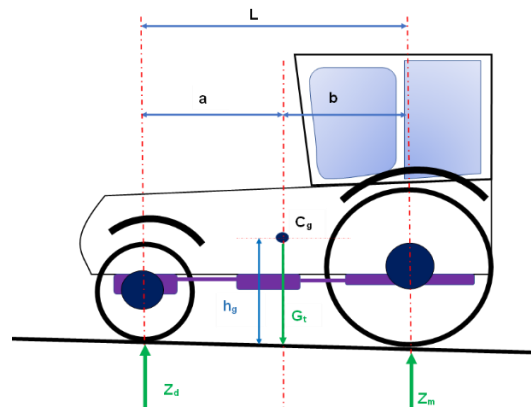


Figure 3.8 Example of transferring the mass of a tractor to the ground

For calculating the masses that are transmitted through the axles, the following relationship is used: [36]

$$m_1 = \frac{b}{L} m_a \quad (3.79)$$

$$m_2 = \frac{a}{L} m_a \quad (3.80)$$

For the calculation of the weights, the relationships are used:

$$Z_d = \frac{l_2}{L} G_t \quad (3.81)$$

$$Z_m = \frac{l_1}{L} G_t \quad (3.82)$$

3.10 The dynamics of the tractor

3.10.1. Dynamics of the 4x2 tractor

Figure 3.9 shows the analysis of a tractor that has a more common transmission, namely 4x2, traveling on an uphill slope. The forces that occur in this situation are shown in the figure below.

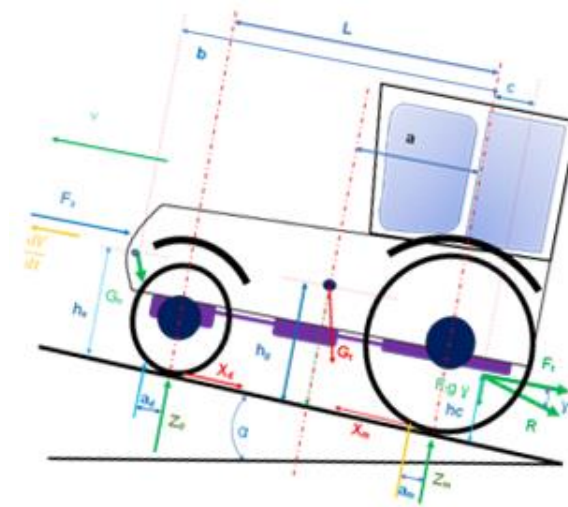


Figure 3.9 Forces present in a tractor with 4x2 transmission.

The motion equations of the tractor are as follows:

$$\frac{G_t}{g} \frac{dV}{dt} = X_m - (G_t + G_l) \sin \alpha - F_t - X_d - R_d \quad (3.83)$$

$$0 = Z_m + Z_d - (G_t + G_l) \cos \alpha - F_t \tan \gamma \quad (3.84)$$

In these equations, the motor torque is not explicitly present, but it can be determined from the tangential reaction on the motor bridge.

From the relationships describing wheel dynamics, the following can be written:

$$M_m = X_m r_m + Z_m a_m + M_{fm} + J_m \frac{d\omega_m}{dt} \quad (3.85)$$

$$X_c r_d = Z_c a_c + M_{fd} + J_c \frac{d\omega_c}{dt} \quad (3.86)$$

Resulting in:

$$X_m = \frac{M_m}{r_m} - Z_m \frac{a_m}{r_m} - \frac{M_{fm}}{r_m} - J_m \frac{d\omega_m}{dt} \frac{1}{r_m} \quad (3.87)$$

$$X_d = Z_d \frac{a_d}{r_d} + \frac{M_{fd}}{r_d} + J_d \frac{d\omega_d}{dt} \frac{1}{r_d} \quad (3.88)$$

To write the equation for tractor traction force, it is noted:

$$\frac{a_m}{r_m} = f_m \quad (3.89)$$

$$\frac{a_d}{r_d} = f_d \quad (3.90)$$

$$f_m = f_d = f \quad (3.91)$$

Resulting in:

$$F_m = \frac{M_m}{r_m} = ((G_t + G_l) \cos \alpha + F_t t g \gamma) f + F_t + (G_t + G_l) \sin \alpha + F_a + \left(\frac{G_t}{g} \frac{dv}{dt} + J_m \frac{d\omega_m}{dt} \frac{1}{r_m} + J_d \frac{d\omega_d}{dt} \frac{1}{r_d} \right) + \left(\frac{M_{fm}}{r_m} + \frac{M_{fd}}{r_d} \right) \quad (3.92)$$

$$F_r = [(G_t + G_l) \cos \alpha + F_t t g \gamma] f \quad (3.93)$$

$$F_\alpha = (G_t + G_l) \sin \alpha \quad (3.94)$$

$$F_j = \frac{G_t}{g} \frac{dv}{dt} + J_m \frac{d}{dt} \frac{1}{r_m} + J_d \frac{d}{dt} \frac{1}{r_d} \quad (3.95)$$

$$F_f = \frac{M_{fm}}{r_m} + \frac{M_{fd}}{r_d} \quad (3.96)$$

After substitution, it results in:

$$F_m = F_r + F_t \pm F_\alpha + F_a \pm F_j + F_f \quad (3.97)$$

The motor power is the product of the motor force and the theoretical velocity, using the following relations, according to equations 3.24, 3.25, and 3.54:

$$\sigma = \frac{v_{pat}}{v_t} = \frac{v_t - v_r}{v_t} = \frac{\Delta r_d}{r_d} \quad (3.98)$$

$$v_r = v_t (1 - \sigma) \quad (3.99)$$

$$P_m = M_m \omega_m = F_m r_m \omega_m = F_m v_t = F_m (v_r + v_{pat}) = F_m v_r + F_m v_{pat} \quad (3.100)$$

$$P_m = F_m v_t = F_m (v_r + v_{pat}) = F_m v_t \frac{v_{pat}}{v_t} = F_m v_r + P_m \delta \quad (3.101)$$

The power lost due to slippage is $P_\delta = P_m \cdot \delta$. According to the above relations, the following relationships can be written:

$$P_m = F_r v_r + F_t v_r \pm F_\alpha v_r + F_a v_r \pm F_j v_r + F_f v_r + P_\delta \quad (3.102)$$

In the above equation, the following are highlighted:

1. Power required to overcome rolling resistance,

$$F_r v_r = P_r \quad (3.103)$$

2. Power required for tractor movement,

$$F_t v_r = P_t \quad (3.104)$$

3. Power used for climbing slopes,

$$F_\alpha v_r = P_\alpha \quad (3.105)$$

4. Power used to overcome air resistance,

$$F_a v_r = P_a \quad (3.106)$$

5. Power used for accelerating the tractor,

$$F_j v_r = P_j \quad (3.107)$$

6. Power lost due to bearing friction,

$$F_f v_r = P_f \quad (3.108)$$

7. Power lost to slippage,

$$P_m \delta = P_\delta \quad (3.109)$$

Due to the low travel speeds in tractors, air resistance is neglected, and the bearing friction is also reduced, which is why it is neglected. Therefore, the balance of forces and powers can be written in the following form:

$$F_m = F_r + F_t \pm F_\alpha \pm F_j \quad (3.110)$$

$$P_m = P_r + P_t \pm P_\alpha \pm P_j + P_\delta \quad (3.111)$$

To allow the tractor to move, the following conditions must be met:

$$F_m = \varphi_m Z_m \leq \varphi_a Z_m = F_{m \max} \quad (3.112)$$

Or:

$$\varphi_m = \frac{F_m}{Z_m} \leq \varphi_a \quad (3.113)$$

In the calculations, the distances a_m and a_d are neglected due to their small size compared to the wheelbase. For constant speed travel, the following results:

$$Z_m L + G_l \cos \alpha (b - L) - G_t \cos \alpha (L - a) - G_t \sin \alpha h_g - G_l \sin \alpha h_1 - F_t t g \gamma (L + 0) - F_t h_c = 0 \quad (3.114)$$

Resulting in:

$$Z_m = \frac{G_t [(L-a) \cos \alpha + h_g \sin \alpha] + G_l [h_1 \sin \alpha - (b-L) \cos \alpha]}{L} + \frac{F_t [(L+0) t g \gamma + h_c]}{L} \quad (3.115)$$

The coefficient of total weight distribution is:

$$\lambda_m = \frac{Z_m}{G_t + G_l} \quad (3.116)$$

When the tractor is in motion, the dynamic coefficient of total weight distribution on the motor axles is defined:

$$\lambda_{mdm} = \frac{G_t [(L-a) \cos \alpha + h_g \sin \alpha] + G_l [h_1 \sin \alpha - (b-L) \cos \alpha]}{L(G_t + G_l)} + \frac{F_t}{G_t + G_l} \frac{(L+0) t g \gamma + h_c}{L} \quad (3.117)$$

When the tractor is not moving, the static coefficient of total weight distribution on the motor axle is defined:

$$\lambda_{msc} = \frac{G_t [(L-a) \cos \alpha + h_g \sin \alpha] + G_l [h_1 \sin \alpha - (b-L) \cos \alpha]}{L (G_t + G_l)} \quad (3.118)$$

To ensure that the tractor moves, the condition must be met:

$$Z_d \geq Z_{d \text{ nec}} \quad (3.119)$$

From studies and experiments, it has been determined that the value of $Z_{d \text{ nec}}$ is around 10% of the total weight of the tractor.

$$Z_{d \text{ nec}} = 0,1 (G_t + G_l) \quad (3.120)$$

From:

$$0 = G_t + Z_d - (G_t + G_l) \cos \alpha - F_t t g \gamma \quad (3.121)$$

It results:

$$Z_d = (G_t + G_l) \cos \alpha + F_t t g \gamma - Z_m \quad (3.122)$$

If we consider relation (3.110), it results:

$$Z_d = (G_t + G_l)(\cos \alpha - \lambda_d) + F_t t g \gamma \quad (3.123)$$

When the values of λ_d are high, it means that it is possible to have high motor forces and, therefore, high traction forces. However, these forces can have a negative impact on tractor maneuverability.

Considering condition (3.113), it results:

$$(G_t + G_l)(\cos \alpha - \lambda_d) + F_t t g \gamma \geq Z_{d \text{ nec}} \quad (3.124)$$

$$\lambda_d \leq \frac{(G_t + G_l) \cos \alpha + F_t t g \gamma - Z_{d \text{ nec}}}{G_t + G_l} = (\cos \alpha - 0,1) + \frac{F_t t g \gamma}{G_t + G_l} \quad (3.125)$$

Replacing λ_d in (3.112) and (3.119) results in:

$$\frac{F_t}{G_t + G_l} \leq \frac{(\cos \alpha - 0,1 - \lambda_d)L}{h_c + c \operatorname{tg} \gamma} \quad (3.126)$$

In conclusion, to maintain tractor maneuverability, the traction force must be limited according to relation 3.120.

According to relations 3.102, 3.116, and 3.111, it can be observed that the presence of additional weight mounted in front of the tractor (ballast) does not contribute to increasing the Z_m , reaction, does not lead to the creation of sufficient conditions for obtaining a high motor force but significantly influences the Z_d reaction.

When the tractor is used for work, it has equipment that may be suspended behind the tractor and in front.

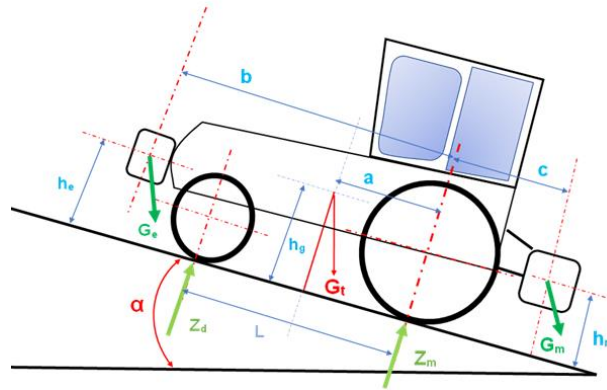


Figure 3.10 The additional forces that occur when additional weights are added

Because of these weights, moments arise, namely the stabilizing and pitching moments that define longitudinal stability (Figure 3.10).

From the condition:

$$Z_d \geq Z_{d \text{ nec}} = 0,1 (G_t + G_l) \quad (3.127)$$

The following relationship for the longitudinal stability coefficient (λ) results:

$$\lambda = \frac{M_s}{M_c} = \frac{G_t \cos \alpha a + G_l \cos \alpha b}{G_m \cos \alpha l_m + G_m \sin \alpha h_m + G_t \sin \alpha h_g + G_l \sin \alpha h_l} \quad (3.128)$$

$$Z_d = \frac{G_t \cos \alpha a + G_l \cos \alpha h_m - G_m \cos \alpha h_m - G_t \sin \alpha h_g - G_l \sin \alpha h_c}{L} \quad (3.129)$$

$$Z_d = \frac{G_t \cos \alpha a + G_l \cos \alpha b - \frac{G_t \cos \alpha a + G_l \cos \alpha b}{\lambda}}{L} \quad (3.130)$$

$$\lambda_{lim} = \frac{G_t \cos \alpha a + G_l \cos \alpha b}{G_t(a \cos \alpha - 0,1L) + G_l \cos \alpha b} \quad (3.131)$$

When calculating the stability coefficient, the ballast is not considered, that is, $G_l=0$, $\alpha=0$ and $a=L/3$.

Thus, the maximum weight of the vehicle, including additional weights, can be calculated as:

$$G_m \leq \frac{(G_t a + G_l b) \cos \alpha - \lambda \sin \alpha (G_t h_g + G_l h_l)}{\lambda (l_l \cos \alpha + h_m \sin \alpha)} \quad (3.132)$$

3.10.2. The dynamics of tractors that are equipped with 4X4 traction

In tractors equipped with 4x4 traction, the total weight is used to increase ground traction. The forces acting on a 4x4 tractor are identical to those on a 4x2 tractor. To distinguish them, subscripts "front - f" and "rear - s" have been introduced. In this case, the motion equations are as follows:

$$\frac{G_t}{g} \frac{dv}{dt} = X_{m s} + X_{m f} - F_t \quad (3.133)$$

$$0 = Z_{m s} + Z_{m f} - G_t - F_t t g \gamma \quad (3.134)$$

From the relations describing the dynamics of the motor wheel 3.44:

$$M_m = X_m r_m + Z_m a_m + J_m \frac{d\omega_m}{dt} \quad (3.135)$$

The following assumptions are used:

$$r_{m s} = r_{m f} = r_m \quad (3.136)$$

and

$$a_{m s} = a_{m f} = a_m \quad (3.137)$$

Resulting in:

$$X_{m s} = \frac{M_{m s}}{r_m} - Z_{m s} \frac{a_m}{r_m} - \frac{1}{r_m} J_{m s} \frac{d\omega_m}{dt} = F_{m s} - Z_{m s} f_m - \frac{1}{r_m} J_{m s} \frac{d\omega_m}{dt} \quad (3.138)$$

$$X_{m f} = \frac{M_{m f}}{r_m} - Z_{m f} \frac{a_m}{r_m} - \frac{1}{r_m} J_{m f} \frac{d\omega_m}{dt} = F_{m f} - Z_{m f} f_c - \frac{1}{r_m} J_{m f} \frac{d\omega_m}{dt} \quad (3.139)$$

$$f_m = \frac{a_m}{r_m} \quad (3.140)$$

If we introduce the two moments of inertia and the rolling resistance coefficient, it results in:

$$F_{m f} + F_{m s} = (Z_{m s} + Z_{m f}) f_m + F_t + \frac{G_t}{g} \frac{dV}{dt} + \frac{1}{r_m} \frac{d\omega_m}{dt} (J_{m f} + J_{m s}) \quad (3.141)$$

Considering the equality from relation 3.131, the traction force balance results:

$$F_{m f} + F_{m s} = (G_t + F_t t g \gamma) f_m + F_t + \frac{G_t}{g} \frac{dV}{dt} + \frac{1}{r_m} \frac{d\omega_m}{dt} (J_{m f} + J_{m s}) \quad (3.142)$$

Or:

$$F_m = F_{m f} + F_{m s} = F_r + F_t \pm F_j \quad (3.143)$$

Regardless of the force developed by the tractor's engine, the adhesion condition must be met. Denoting the effective utilization coefficient of adhesion:

$$\varphi_m = \varphi_{m f} = \varphi_{m s} \quad (3.144)$$

It results:

$$F_{m s} = \varphi_m Z_{m s} \text{ și } F_{m f} = \varphi_m Z_{m f} \quad (3.145)$$

If we consider uniform motion, from relation 3.138 and the adhesion condition, the traction force results as follows:

$$F_t = \varphi_m (G_t + F_t t g \gamma) - f_c (G_t + F_t t g \gamma) \quad (3.146)$$

After simplification, it results:

$$F_t = G_t \frac{\varphi_m - f_m}{1 - (\varphi_m - f_m) t g \gamma} \quad (3.147)$$

Under identical working conditions, the same type of tractor with either 4x2 or 4x4 traction will develop a higher traction force when equipped with 4x4 traction.

If:

$$t g \gamma = 0 \quad (3.148)$$

$$F_{t 4x4} = (\varphi_m - f_m) G_t \quad (3.149)$$

and

$$F_{t 4x2} = (\varphi_m \lambda_m^{-f} \lim) G_t \quad (3.150)$$

It results:

$$\frac{F_{m\ 4X4}}{F_{m\ 4X2}} = \frac{\varphi_m^{-f}}{\varphi_m \lambda_m^{-f}} \quad (3.151)$$

When using typical values, $\varphi_m = 0,6$ și $f = 0,1$ it results:

$$\frac{F_{m\ 4X4}}{F_{m\ 4X2}} = 1,3 \quad (3.152)$$

From the above relationship, it can be observed that when using 4x4 traction, for the same engine power, a 30% higher traction force is obtained.

Previously, the conditions: $a_{mf} = a_{ms}$, $\varphi_{mf} = \varphi_{ms}$, $f_{mf} = f_{ms}$, $r_{mf} = r_{ms}$ led to $Z_{mf} = Z_{ms}$.

In these conditions, the relation is:

$$Z_{ms} = Z_{mf} = \frac{G_t + F_t t g \gamma}{2} \quad (3.153)$$

The equation that defines the moments appearing with respect to the wheel axis and the ground contact points for the rear wheels is:

$$\frac{G_t + F_t t g \gamma}{2} (2a_m + L) + F_t (h_c + c t g \gamma) - G_t a = 0 \quad (3.154)$$

Where:

$$a = \frac{L}{2} + a_m + \frac{F_t}{2 * G_t} [t g \gamma (2a_m + 2c + L) + 2h_c] \quad (3.155)$$

It can be observed that $b > L/2$, in conclusion, the center of gravity is located towards the front of the tractor.

If we denote v_{tf} and v_{ts} as the theoretical speeds at the front and rear wheels, in this case, slip coefficients for the front and rear wheels, δ_f and δ_s , appear.

Thus, the actual speed can be defined as:

$$v_r = v_{ts} (1 - \delta_s) = v_{tf} (1 - \delta_f) \quad (3.156)$$

Since the speeds are:

$$v_{ts} = r_{ms} \omega_s \text{ și } v_{tf} = r_{mf} \omega_f \quad (3.157)$$

It results:

$$\frac{r_{ms} + \omega_s}{r_{mf} + \omega_f} = \frac{1 - \delta_f}{1 - \delta_s} \quad (3.158)$$

$$k_{cin} = \frac{\omega_s}{\omega_f} \quad (3.159)$$

$$k_r = \frac{r_{ms}}{r_{mf}} \quad (3.160)$$

When the wheels have equal radii, $k_{cin} = 1$, which results in:

$$k_r = \frac{1 - \delta_f}{1 - \delta_s} \quad (3.161)$$

From the above relationship, a connection between the slip coefficients between the front and rear axles is:

$$\delta_s = \left(1 - \frac{1}{k_r}\right) + \frac{\delta_f}{k_r} \quad (3.162)$$

The condition for a tractor to function is that $\delta_f = 0$ and $k_r = 1$; when $k_r > 1$, the rear wheels slip.

$$\delta_s < 1 - \frac{1}{k_r} \quad (3.163)$$

When $\delta_f < 0$ front wheels slip. In this case, the front axle loses the ability to overcome resistance forces, which are taken over by the forces acting through the rear wheels.

In practice, the appearance of parasitic forces causes a 4x4 transmission tractor to behave, for a limited period, like a 4x2 transmission tractor.

There is also a case where $k_r < 1$ and $\delta_s < 0$. In this case, slipping occurs at the rear wheels when the tractor has unequal wheel radii, and k_r and $k_{min} \neq 1$. The technical solution in this case was to introduce a unidirectional coupling at the front axle.

3.11. Longitudinal stability

By definition, longitudinal stability is the tractor's ability to stand still while braking or to perform uniform motion during work on a line with the steepest slope of an inclined terrain without overturning (Figure 3.11).

Longitudinal stability can be expressed by the value of the reaction on the upstream axle, which must be equal to zero, greater, or at the limit.

Specifically, for $Z_d \geq 0$,

$$F_m v_t = F_m (v_r + v_{pat}) = F_m v_r + F_m v_t \frac{v_{pat}}{v_t} = F_m v_r + P_m \delta \quad (3.164)$$

Resulting in:

$$Z_d = \frac{G_t a \cos \alpha - G_t h_g \sin \alpha}{L} \geq 0 \quad (3.165)$$

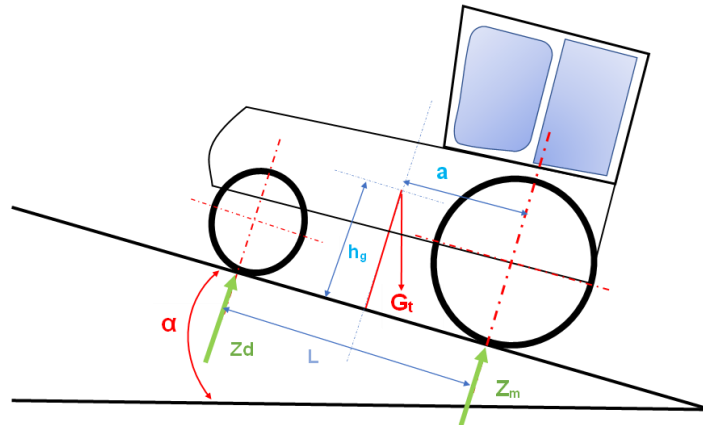


Figure 3.11 Longitudinal stability forces

Resulting in:

$$\operatorname{tg} \alpha_u \leq \frac{l_2}{h_g} \quad (3.166)$$

To determine the maximum incline angle that can be climbed, the following equation must be true:

$$\operatorname{tg} \alpha_{max u} = \frac{l_2}{h_g} \quad (3.167)$$

When the tractor descends a slope, there is no traction force under the condition:

$$Z_m \geq 0$$

$$Z_m = \frac{G_t (L-a) \cos \alpha - G_t h_g \sin \alpha}{L} \geq 0 \quad (3.168)$$

This results in:

$$\operatorname{tg} \alpha_c \leq \frac{L-a}{h_g} \quad (3.169)$$

The maximum slope angle for descending is defined by:

$$\operatorname{tg} \alpha_{\max c} = \frac{L-a}{h_g} \quad (3.170)$$

The stability condition is:

$$Z_d \geq 0 \quad (3.171)$$

Or:

$$Z_d = \frac{G_t a \cos \alpha - G_t h_g \sin \alpha - F_t h_c - F_t \operatorname{tg} \gamma a}{L} \geq 0 \quad (3.172)$$

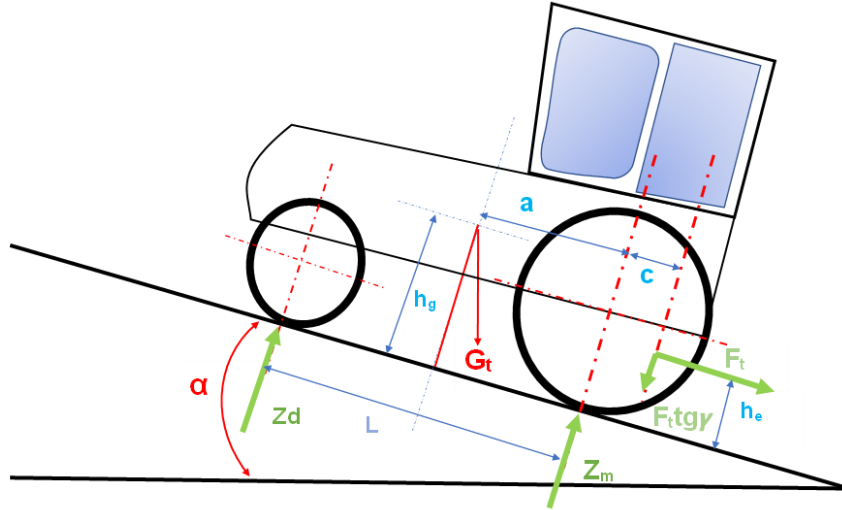


Figure 3.12 Stability of the tractor on the slope with traction force

From the traction force balance equation and under the assumption that F_a , F_j , and F_f can be neglected, it follows:

$$F_t = F_m - F_r - F_\alpha = \varphi \lambda_d G_t \cos \alpha - f(G_t \cos \alpha + F_t \operatorname{tg} \gamma) - G_t \sin \alpha \quad (3.173)$$

And

$$F_t = \frac{G_t(\varphi_0 \lambda_m \operatorname{lim} \cos \alpha - f \cos \alpha - \sin \alpha)}{1 + f \operatorname{tg} \gamma} \quad (3.174)$$

If we introduce it into 3.113, the condition can be derived:

$$\operatorname{tg} \alpha \leq \frac{a(1 + f \operatorname{tg} \gamma) - (h_c + c \operatorname{tg} \gamma)(\varphi_0 \lambda_m \operatorname{lim} - f)}{h_g(1 + f \operatorname{tg} \gamma) - (h_c + c \operatorname{tg} \gamma)} \quad (3.175)$$

In conclusion:

$$\operatorname{tg} \alpha_{\max \text{ din } u} = \frac{a(1 + f \operatorname{tg} \gamma) - (h_c + c \operatorname{tg} \gamma)(\varphi_0 \lambda_m \operatorname{lim} - f)}{h_g(1 + f \operatorname{tg} \gamma) - (h_c + c \operatorname{tg} \gamma)} \quad (3.176)$$

When $\gamma = 0$ it results in:

$$\operatorname{tg} \alpha_{\max \text{ din } u} = \frac{a - h_c(\varphi_0 \lambda_m \operatorname{lim} - f)}{h_g - h_c} \quad (3.177)$$

3.12. Transverse stability

Transversal stability of the tractor prevents overturning. For this, it is necessary for the reactions on the right and left wheels to be greater than zero (Figure 3.13).

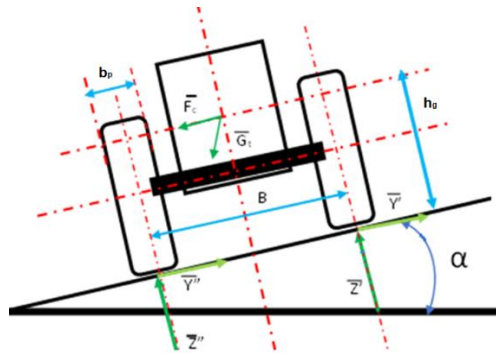


Figure 3.13 The forces that occur when the tractor is tilted transversely

In Figure 3.13, the forces that occur during the lateral tilting of the tractor are depicted. The stability condition is $Z' \geq 0$. When the vehicle is stationary or moving uniformly in a straight line, the relationship can be written as:

$$Z' = \frac{G_t \cos \alpha B - 2G_t \sin \alpha h_g}{2B} \geq 0 \quad (3.178)$$

And:

$$\text{tg } \alpha_{tr} \leq \frac{B}{2h_g} \quad (3.179)$$

The tipping situation occurs when the vehicle makes an upstream turn, in which case the centrifugal force contributes to tipping.

In this case, we have:

$$Z' = \frac{G_t \cos \alpha B - 2G_t \sin \alpha h_g - 2F_c h_g}{2B} \geq 0 \quad (3.180)$$

Practically, the tipping angle is calculated using the following relationship:

$$G_t B \cos \alpha - 2G_t h_g \sin \alpha - 2F_c h_g \geq 0 \quad (3.181)$$

To find the maximum value of the angle of inclination, the function is solved:

$$f(\alpha) = \frac{G_t(B \cos \alpha - 2h_g \sin \alpha)}{2h_g} \quad (3.182)$$

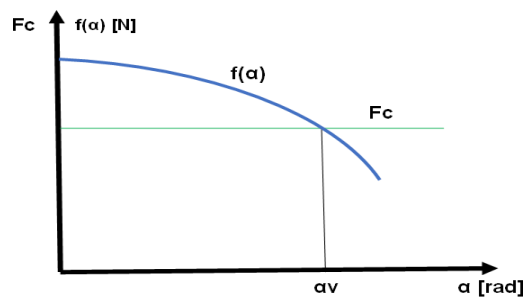


Figure 3.14 The transverse stability characteristic

The graph of the function $f(\alpha)$ is shown in figure 3.14. It can be seen that the maximum angle of transverse stability is also influenced by the traction force.

Chapter 4 The current state of construction of tractors and chassis intended for equipping with electric motors

4.1 The propulsion system of tractors equipped with internal combustion engines

4.1.1 The engine

The types of engines existing on tractors have been inventoried, and the essential specifications needed for these engines to provide specific power to each type of tractor have been identified.

The engine serves as the power source for the tractor, converting the thermal energy generated from the combustion of fossil fuel or biofuel into mechanical energy required for the tractor's movement and the operation of the attached machinery.

The thermal engines used in tractors include:

- Internal combustion engines, which use either liquid or gaseous fuels;
- Gas turbine engines;
- Steam engines. [37]

Figure 4.1 presents the variation of torque and power in internal combustion engines as general, non-specific graphs applicable to various engine types.

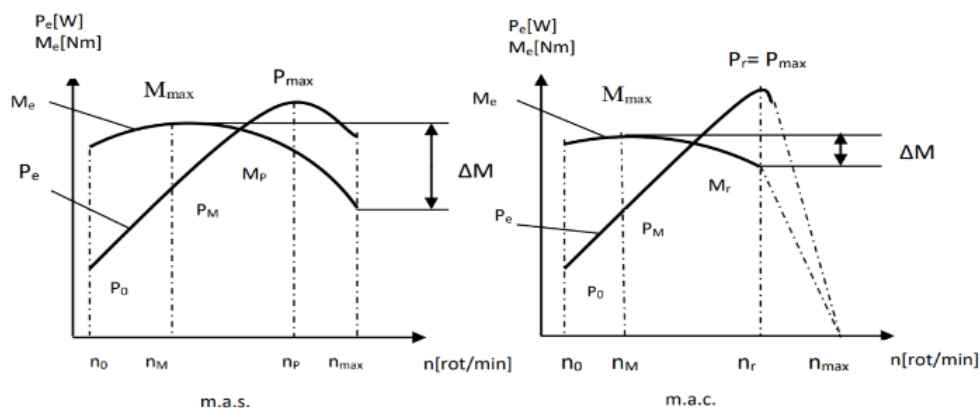


Figure 4.1 Variation of torque and power as a function of speed [38]

The torque and power curves presented are generic and do not belong to a specific engine. Additionally, the shape of these curves depends on the engine type (gasoline or diesel), the type of air intake system (naturally aspirated or supercharged), or the injection type (direct or indirect).

4.1.2 Transmission

The tractor's transmission can be represented as the sum of mechanisms through which the engine power is transferred to the wheels or tracks.

Based on the type of transmission, tractors can be categorized as:

- Mechanical transmission (in gears or continuously variable);
- Hydrostatic transmission;
- Hydrodynamic transmission;
- Electric transmission;
- Combined transmission (electromechanical). [37]

4.2. The components of the electric propulsion systems

4.2.1. Types of electric motors

During the experiments, four types of engines were studied, and their characteristics are presented below.

The **AME200.0114** engine, with a power of 16 kW, is a three-phase asynchronous motor, powered by a 144 V battery (Figure 4.2).



Figure 4.2 AME200 engine produced by C.F.R. LLC Italy [41]

The **10 kW YS210H1096H61-LU** motor (figure 4.3) powered at 96 Vcc.



Figur3 4.3 10 kW motor

The **ME1115** motor (figure 4.4) produced by Motenergy. [43]

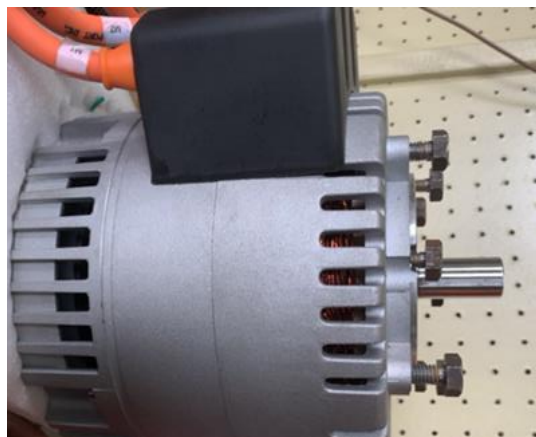


Figure 4.4 ME1115 motor

The **ME 0907** motor can be powered with voltages between 24 and 48 Vdc (figure 4.5).

[44]



Figure 4.5 6kW ME 0907 motor

4.2.2. Types of accumulator batteries

The 144 V battery, model **PMI1-120S3P-1069-00000** (figure 4.6), is constructed from 3.7 V Li-Ion cells that are connected in series.



Figure 4.6 144V battery model PMI1-120S3P-1069-00000

The **96V battery** (figure 4.7) consists of Li-Ion batteries with a cell voltage of 3.7 V and 70 Ah, with a maximum capacity of 9 kWh.

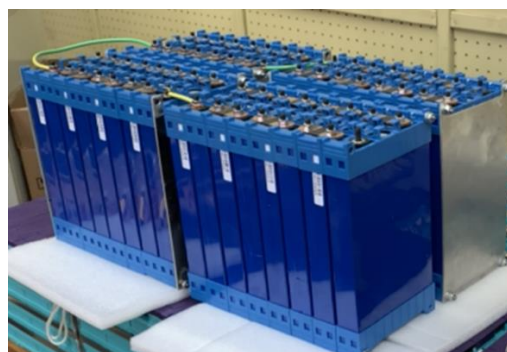


Figure 4.7 96V battery

Another battery model also of 96 V and 70 Ah is shown in figure 4.8.



Figure 4.8 9 kW battery

4.2.3. Types of motor controllers

During the experiments, 4 types of battery controllers were studied, whose characteristics are presented below.

The **KellyControllers KAC-8080I** motor controller (figure 4.9).



Figure 4.9 Kelly KAC-8080I controller[46]

Kelly KLS 7245 motor controller (figure 4.10).



Figure 4.10 Kelly KLS 7245 controller[46]

The motor controller, **Curtis 1239e**, shown in figure 4.11.



Figure 4.11 Curtis 1239e controller[50]

SEVCON GEN 4 motor controller, shown in figure 4.12.



Figure 4.12 Sevcon Gen 4 controller

4.2.4. Types of DC/DC converters

During the experiments, 3 types of DC-DC converters were studied, whose characteristics are presented below.

The **Mean Well 1000W DC/DC** converter, as shown in Figure 4.13.



Figure 4.13 DC/DC converter from 144 V to 12 V 1000 W Mean Well [52]

300 W DC/DC Converter (Figure 4.14).



Figure 4.14 DC/DC Converter

The DC/DC converter **EICon 500W** (figure 4.15).



Figure 4.15 500W EICon DC/DC converter

4.2.5. Types of chargers

The **HK-J charger 6.6 kW** series (figure 4.16).



Figure 4.16 6.6 kW charger

The **TC charger 3.3 kW** (figure 4.17).



Figure 4.17 Charger 3.3 kW

The **3.3kW EICon** charger (figure 4.18).



Figure 4.18 EICon charger 3.3 kW [58]

4.2.6. Types of battery management systems (BMS)

The Orion 2 BMS (figure 4.19).



Figure 4.19 BMS Orion 2 [60]

The **BMS G1** Control Unit (figure 4.20).



Figure 4.20 BMS EMUS G1

Chapter 5 Experimental research on the realization of electrically driven agricultural vehicles

5.1. Analysis of the possibility of replacing an internal combustion engine with an electric one and studying the required equipment

One of the doctoral thesis's objectives was to investigate the possibility of replacing an internal combustion engine with an electric one in the case of an electric tractor. Consequently, it was necessary to overcome some technically challenging issues related to adaptation and conversion to electric propulsion to achieve this goal.

The first problem that needed to be overcome was the physical connection of the electric motor to the vehicle's propulsion system. Various methods were tested to find a solution that would be safe, especially for the personnel operating this vehicle. The research into this mounting method aimed to minimize modifications to the vehicle's chassis as much as possible. This was done to reduce the budget needed for this type of modification (Figures 5.1 and 5.2).



Figure 5.1 The mounting system of the electric motor to the chassis of the electric vegetable tractor



Figure 5.2 Mounting the engine on the chassis

From the study conducted on tractor chassis, it was found that, in general, the chassis structure integrates even the engine block of the internal combustion engine. This posed a series of complications related to the design of the tractor's structural framework because the electric motor is not designed to withstand the torsional and shear forces of the magnitude present in the structural framework of a tractor.

These problems were addressed through the design and construction of a new chassis segment capable of withstanding such forces and moments (Figure 5.3).



Figure 5.3 Experiments in the realization of the new chassis of the electric tractor

While the battery is bulky and has a substantial mass, ranging from 100 to 300 kg depending on the number of cells, it has an extraordinary advantage. Specifically, it can be mounted on a structure that can be easily moved along the longitudinal plane of the electric tractor. This offers the chance to adjust the tractor's center of gravity as needed without additional weights on the tractor. This arrangement ensures consistent consumption and improved traction (Figures 5.4, 5.5, and 5.6).



Figure 5.4 Experiments with the structure on which the battery will be mounted and the electronic engine control system



Figure 5.5 Details of the battery and electronic engine control system mounting system



Figure 5.6 Battery holder and electronic control system completed

At the end of the experiments, the assembly solutions for the electric motor, control system and battery were accepted (figure 5.7).



Figure 5.7 Detail from the installation of the electronic equipment on the electric tractor

The final conclusion of these experiments was that an electric motor can be fitted instead of a thermal one with a small number of changes to the chassis.

5.2. Tractor chassis used for experimentation

5.2.1 Vegetable chassis

For the experiments, four chassis were used, designed and made within the INMA Bucharest.

1. Electric vegetable tractor

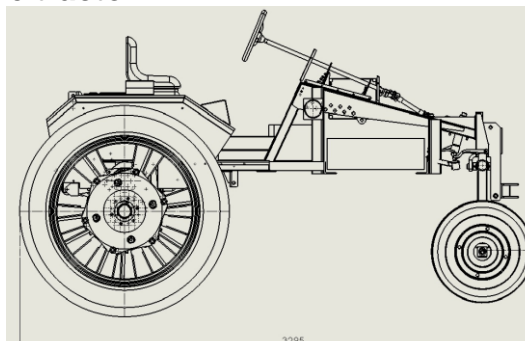


Figure 5.8 Sketch of the electric vegetable tractor chassis

2. General purpose electric tractor, low power tractor.

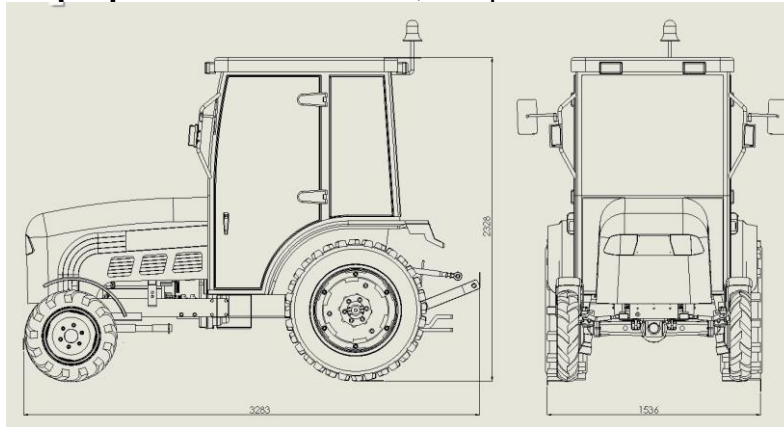


Figure 5.9 Sketch of the electric tractor

3. The electric tractor for transporting agricultural products.



Figure 5.10 Electric transport tractor

4. Electric vehicle chassis for spraying work.



Figure 5.11 The electric vehicle intended for spraying work in field tests

5.4. Devices, apparatus, and methods of setting, adjusting, and measuring used

5.4.1. Programming and control interfaces

- The 1313 mobile programmer;
- IXXAT interface, USB-to-CAN V2;
- Clearview-display;

5.4.2. PC software needed for programming, configuration and control

- 1314 interface;
- Curtis Integrated Toolkit V1.5 (CIT);
- Orion BMS 2 Utility;
- canAnalyser;
- EMUS BMS Control Panel;
- KMC User App;

5.4.3. The equipment used for measurements and control

- Amarell Digital Thermometer;
- Digital scale CAS RW 2601P;
- MatrixPro 570G GPS;
- Bruel & Kjaer sound level meter, type 2237;
- DOSTMANN thermohygrometer, type P330;
- Cole-Parmer type CIH20DL anemometer;
- QuantumX MX1615B / MX1616B;

5.5. Determinarea caracteristicilor fizice ale vehiculele agricole acționate electric

5.5.1. Determination of the mass of electric vehicles

The mass of the agricultural vehicles was determined by weighing them using RW10P platform scales, with an air temperature of 25.6°C, atmospheric pressure of 747.1 mm of mercury, and a relative humidity of 58%. The result of this determination is presented in Table 5.1.

Table 5.1 Masses of electric vehicles from experiments.

No.	Characteristic	M.U.	The value of the parameters determined in tests
1.	Total mass of electric vegetable tractor	kg	1450
2.	Total mass of electric tractor	kg	1970
3	The total weight of the electric vehicle for spraying	kg	1283
4	Total mass of the electric transport tractor	kg	1379

5.5.2. Determining the motor shaft speed

The RPM measurement was carried out using a tachometer on the electric tractors under stationary conditions, and RPM values remarkably close to 2300 RPM were recorded, with variations of up to $\pm 2\%$. During motion, the RPM did not remain constant due to the

influence of inertia forces and resistance to movement, resulting in RPM variations of up to $\pm 20\%$ compared to the established maximum RPM.

Table 5.2 RPM measurements on the tractors used in the trials.

No.	Characteristic	M.U.	Test-determined RPM		
			Stationary (rpm)	Minimum values on the move (rpm)	Maximum values on the move (rpm)
1.	Engine speed measured, electric tractor	<i>rpm</i>	2347	1900	2540
2	Engine speed measured, electric vegetable tractor	<i>rpm</i>	2334	1923	2533
3	Engine speed measured, electric vehicle for spraying	<i>rpm</i>	2348	1892	2485
4	Engine speed measured, electric transport tractor	<i>rpm</i>	2325	1897	2379

5.5.3. Determination of battery charging time

The charging time for the three types of batteries was measured using a multimeter and a stopwatch, as well as with the help of the PC communication interface connected to the Battery Management System (BMS). The charging times corresponding to the three power modes were determined.

The 17 kWh battery (Figure 4.6) was mounted on the general-purpose electric tractor and the vegetable electric tractor, the 9 kWh type 1 battery (Figure 4.7) was mounted on the transport electric tractor, and the 9 kWh type 2 battery (Figure 4.8) was mounted on the electric vehicle for spraying.

Table 5.3 Charging time required for the batteries.

Battery Type	Characteristic	M.U.	The charging time determined in the tests		
17 kWh battery	Power from 220 V 6 A	<i>Minutes</i>	648	660	667
17 kWh battery	Power from 220 V 16 A	<i>Minutes</i>	263	251	248
17 kWh battery	Power from 220 V 32 A	<i>Minutes</i>	132	127	124
9 kWh type 1 battery	Power from 220 V 6 A	<i>Minutes</i>	432	426	426
9 kWh type 1 battery	Power from 220 V 16 A	<i>Minutes</i>	163	164	162
9 kWh type 1 battery	Power from 220 V 32 A	<i>Minutes</i>	78	79	77
9 kWh type 2 battery	Power from 220 V 6 A	<i>Minutes</i>	426	438	426
9 kWh type 2 battery	Power from 220 V 16 A	<i>Minutes</i>	166	168	166
9 kWh type 2 battery	Power from 220 V 32 A	<i>Minutes</i>	82	81	83

5.5.4. Determining the masses of the tractors

Table 5.5 shows the masses of the electric tractors used in the experiments and their distribution between the front and rear axles.

Table 5.5 Shows the distribution of masses on the front and rear axles of the electric tractors used in the experiments.

Tractor type	The total mass of the tractor during the tests (kg)	Front wheel mass (kg)	Rear wheel mass (kg)
Electric vegetable tractor	1450	500	950
Electric tractor	1970	750	1220
Electric vehicle for spraying	1270	427	843
Electric transport tractor	1430	489	941

5.5.5. Braking Safety Assessment

Test Conditions - following Regulation (EU) No. 167/2013 of the European Parliament and of the Council on the approval and market surveillance of agricultural and forestry vehicles. The results are presented in tables 5.6 and 5.7.

Table 5.6 Brake test results. Brake type: with cold brakes

Determined parameters		Maximum permissible values	Determined values, Electric tractor	Determined values, electric vegetable tractor	Determined values, electric vehicle for spraying	Determined Values Electric Transport Tractor
Initial speed	[km/h]	40 + 3	27,8	30,2	33,7	29,7
	m/s	11,1	7,72	8,38	9,36	8,25
Average deceleration [m/s ²]		-	2,91	3,82	2,94	3,79
Maximum deceleration [m/s ²]		-	8,61	10,40	7,71	9,86
Braking distance (m)	calculated	$x < 0,15v + v^2/116$	10,73	12,43	10,84	12,35
	experimentally determined	-	8,17	9,63	7,69	9,07
Total braking time [s]		-	2,39	4,21	2,31	4,11
Actuation force at the pedal [daN]		max 60	54,75	56,04	55,04	56,03

Table 5.7 Braking test results. Brake type: with hot brakes

Determined parameters		Maximum permissible values	Determined values, Electric tractor	Determined values, electric vegetable tractor	Determined values, electric vehicle for spraying	Determined Values Electric Transport Tractor
Initial speed	[km/h]	40 + 3	27,8	30,2	33,7	29,7
	m/s	11,1	7,72	8,38	9,36	8,25
Average deceleration [m/s ²]		-	3,11	4,28	2,81	4,30
Maximum deceleration [m/s ²]		-	8,64	10,73	7,59	10,81
Braking distance (m)	calculated	$1/x < (0,15v + v^2/116) * 75\%$	11,97	13,87	10,72	13,72
	experimentally determined	-	8,28	10,31	7,34	10,28
Total braking time [s]		-	2,34	4,37	2,27	4,35
Actuation force at the pedal [daN]		max 60	56,8	56,24	54,9	56,29

5.5.5. Determining the level of acoustic pressure around the tractor and at the tractor driver's ear

The noise of the tractor is the sum of noises generated by the engine, exhaust, cooling fan, and the mechanical noise created by transmissions and accessories. The noise spectrum covers the frequency range from 20 Hz to 20 kHz. A noisy tractor can be a source of stress, lead to a lack of concentration, fatigue, and hearing damage.

The data obtained from experiments are recorded in Table 5.8.

Table 5.8 Noise Level Around the Tractor.

Parameter	Allowed values	Values determined electric tractor	Values Determined electric vegetable tractor	Values Determined electric transport tractor	Values Determined electric vehicle for spraying
Test Entry Speed/Test Speed (km/h)	the gear corresponding to $\frac{3}{4}$ of V_{max} but with the engine unpacked / the same gear with the engine packed at maximum	approx. 19.83/28 (IV gear)	approx. 27,60/30 (II gear)	approx. 27,60/30 (III gear)	approx. 33,4/30 (II gear)
External noise level (dB)	89 for $m_t > 1,5$ t	62.6 Left 81.9 right	59,1 Left 60,03 right	58,8 Left 59,6 right	57,7 Left 57,8 right

It has been observed that there are differences between the right and left sides of the vehicles regarding the generated noise. This is due to the hydraulic system's position, responsible for power steering and operating the attachments that can be connected to the tractor.

The noise levels measured inside the cabin at the operator's ear level are presented in Table 5.9.

Table 5.9 Noise Level Measured at the Operator's Ear Level.

Parameter	Allowed values	Values determined electric tractor	Values Determined electric vegetable tractor	Values Determined electric transport tractor	Values Determined electric vehicle for spraying
Test speed km/h	7,25	~ 7,25	~ 7,25	~ 7,25	~ 7,25
Noise level at the operator's ear (dB)	max. 86 with windows and doors closed (conf. annex II)	76,8	61,3 (it does not have a cabin)	60,6 (it does not have a cabin)	77,4
	max. 86 with windows and doors open (conf. annex II)	75,9	61,3 (it does not have a cabin)	60,6 (it does not have a cabin)	76,9

The determined values fall within the legal limits; from this perspective, all tractors equipped with electric motors produce noise or acoustic pressure with values far below those generated by a tractor equipped with an internal combustion engine.

5.5.6. Determination of energy indices

5.5.6.1. Determining the speed of movement

The traveling speed is determined by calculation, measuring the time required to cover 50 meters. Three measurements were taken, and the average of the measured data was reported. The speed was calculated using the formula:

$$v = \frac{3,6d}{t} [km/h] \quad (5.1)$$

Table 5.10 Presentation of Results Obtained from Experiments.

No.	Characteristic	M.U.	Maximum speed	Average speed
1	Calculated speed electric tractor	Km/h	28,3	25,1
2	Calculated speed electric vegetable tractor	Km/h	30,2	27,3
3	Calculated speed electric vehicle for spraying	Km/h	40,4	31,7
4	Calculated speed electric transport tractor	Km/h	30,1	26,9

5.5.6.2. Determining the consumption of electrical energy from the grid

The absorbed power (P) from the grid was measured, and the electrical energy consumed was calculated using the formula:

$$W = \frac{P t}{3600} [kWh] \quad (5.2)$$

The charging energy, which ends up being stored in the battery, is determined with an efficiency coefficient of the charger (μ).

$$E_b = W\mu [kW] \quad (5.3)$$

Table 5.11 presents the energy consumption from the grid when charging the batteries mounted on electric tractors, and the charging time is shown in Table 5.3.

Table 5.11 Results obtained from experiments.

Battery Type	Characteristic	M.U.	Energy consumed W	Stored energy W* μ	Charger efficiency coefficient μ	Tractor type
17 kW	Energy consumed at 220 V 6 A	kWh	1320	1227	93%	Electric tractor/Electric vegetable tractor
17 kW	Energy consumed at 220 V 16A	kWh	3520	3273	93%	Electric tractor/Electric vegetable tractor
17 kW	Energy consumed at 220 V 32 A	kWh	7040	6547	93%	Electric tractor/Electric vegetable tractor
9 kW (1)	Energy consumed at 220 V 6 A	kWh	1320	1254	95%	Electric vehicle for spraying
9 kW (1)	Energy consumed at 220 V 16A	kWh	3520	3344	95%	Electric vehicle for spraying
9 kW (1)	Energy consumed at 220 V 32 A	kWh	7040	6687	95%	Electric vehicle for spraying
9 kW (2)	Energy consumed at 220 V 6 A	kWh	1320	1214	92%	Electric transport tractor
9 kW (2)	Energy consumed at 220 V 16A	kWh	3520	3238	92%	Electric transport tractor
9 kW (2)	Energy consumed at 220 V 32 A	kWh	7040	6476	92%	Electric transport tractor

These tests were conducted on the test bench in the INMA Bucharest engine laboratory.

5.5.6.3. Determination of Traction Force

The traction test was conducted on agricultural and asphalt terrain under approximately the same weather conditions.

Table 5.12 Traction forces determined in experiments.

No.	Characteristic	M.U.	Electric tractor Traction force 4X4	Electric tractor Traction force 4X2	Electric vegetable tractor Traction force 4X2	Electric transport tractor Traction force 4X2	Electric vehicle for spraying Traction force 4X2
1.	Traction on asphalt	kN	16,5	15	7,6	5,8	5,2
2.	Traction on agricultural land	kN	21,5	18	14,2	9,3	7,8

5.5.6.4. Determination of Autonomy

It was performed using the state of charge estimation method (SOC), which consists of determining the decrease in electric energy consumption and adding electric energy regeneration. The following parameters are used: SOC_0 at startup (reported by BMS), current SOC (reported by BMS), energy losses, X_0 initial distance in km (recorded on the dashboard), X distance traveled, start time, end time, X_{max} maximum distance.

The estimation of the remaining distance that can be traveled should be done by the on-board computer (CB) and must be visible to the driver. One method is to calculate the remaining range in kilometers using the formula:

$$X_{max} = X + (SOC - SOC_{min}) \frac{X - X_0}{SOC_0 - SOC} \quad (5.4)$$

This method is relative, considering the counter reset at the beginning of each trip as equivalent to a full recharge of the electric vehicle.

The graphs in Figures 5.12 and 5.13 depict the battery current over time, expressed in seconds. For accurate assessment, an integrated value of the current in the last 60 seconds is provided using the "moving average" method. [82]

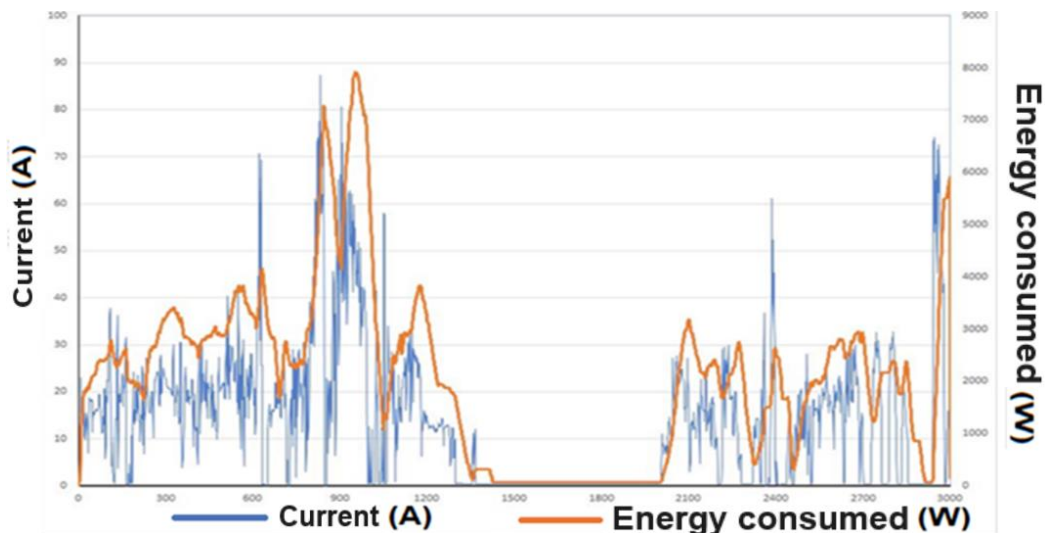


Figure 5.12 Average variation of current and voltage over 60 seconds [83]

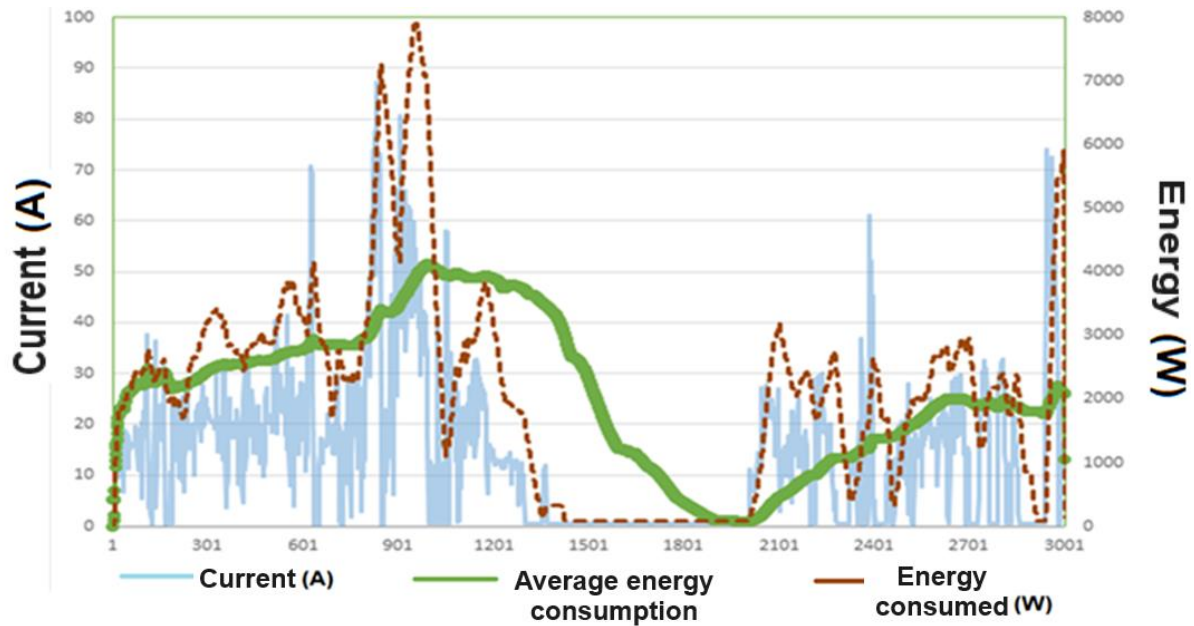


Figure 5.13 Average variation of current and power consumed for 60 seconds [83]

If one intends to deduce the remaining energy for estimating autonomy at moment n , equation (5.6) must be used. As the value of the integrating factor k_n is a divisor, the minimum value for this factor must be considered. In this case, a value of 1054 Wh is considered, chosen as the lowest instantaneous power value when the tractor is moving without a load.

$$t_n = P_{tot} \frac{SOC - SOC_0}{k_n} \quad (5.5)$$

$$k_n = \frac{1}{m \Delta t} \sum_{i=n-m}^n P_i \quad (5.6)$$

Another method for estimating autonomy is based on the energy reserve using predefined measurements and records of consumed energy. The method involves using equation 5.5, and a consumption factor for the minimum load k_{min} and another for the maximum load k_{max} . must be chosen. here are two autonomy results, namely t_{load} , for minimum consumption, and t_{free} , for maximum consumption.

$$t_{free} = P_{tot} \frac{SOC - SOC_0}{k_{min}} \quad (5.7)$$

$$t_{load} = P_{tot} \frac{SOC - SOC_0}{k_{max}} \quad (5.8)$$

Experiments were conducted on the track within INMA Bucharest, on asphalt surfaces, dirt roads, inclined surfaces, and plowing.

Table 5.12 presents the autonomy of electric tractors for various tasks.

Table 5.13 Autonomy of electric agricultural vehicles.

Agricultural work	Autonomy electric tractor (h)	Autonomy electric vegetable tractor (h)	Autonomy electric transport tractor (h)	Autonomy electric vehicle for spraying (h)
Displacement	4,5	5,0	3	4,7
Traction 2000kg	3,8	3,6	2,1	NA
Plowing	1,1	NA	NA	NA

In the experiments aimed at determining the travel range autonomy, a predefined route was used, located within the INMA Bucharest's test track.

5.5.6.5. Fuel Economy

In internal combustion engines, multi-speed gearboxes are used to maintain traction force as constant as possible, allowing for efficient tractor operation. For comparison, data from tractors' specific fuel consumption displayed on the www.cdep.ro website were utilized.

The considerations that formed the basis for selecting the batteries mounted on vehicles were as follows:

1. The ability for them to be charged from a 220 V network with a minimum of 6 A;
2. The energy efficiency of the charging chain should exceed 90 %;
3. The charging device should use a connector also used by other vehicles for connection to the power supply network;
4. The motor controller's efficiency should be over 90 %;

When choosing the battery type, constraints imposed by the motor controllers were considered. For instance, for a 6 kW motor powered at 96 V with a maximum current consumption of 80 A at nominal speed:

$$I_d \geq \frac{P_n}{U_a \eta_e} = \frac{6000}{96 * 0.95} = 65,79 \text{ A} \quad (5.9)$$

According to this calculation, a battery capable of supporting a maximum discharge current of 70 Ah can be selected.

For charging this type of battery, the charging current can be relatively simply calculated using the following relationship:

$$I_c = \frac{I_d}{2} = 35 \text{ A} \quad (5.10)$$

The energy delivered by the battery is:

$$E_a = U_a I_c = 96 * 70 = 6,3 \text{ kWh} \quad (5.11)$$

Thus, it is possible to calculate the energy that can be used, approximately 80% of the total energy of the battery:

$$E_e = E_a * 0,8 = 5,05 \text{ kWh} \quad (5.12)$$

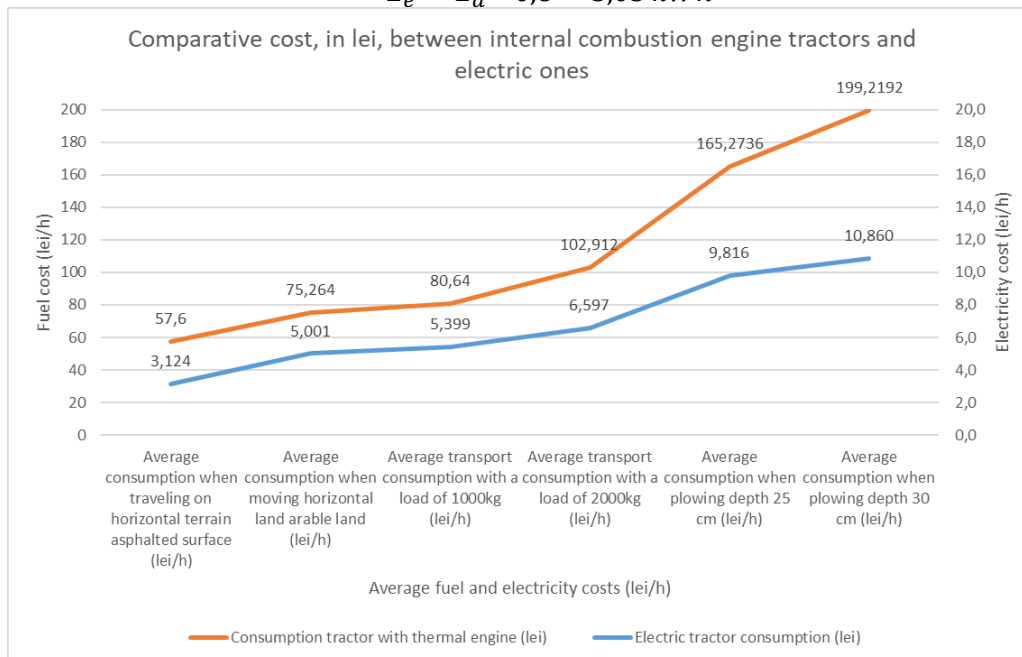


Figure 5.14 Comparison of energy costs between the tractor equipped with an internal combustion engine and the electric tractor.

As evident from the graph (Figure 5.14), the hourly cost in Romanian Lei (RON) for the electric tractor used exclusively for towing, where consumption is at its lowest, i.e., 4.45 kWh and with an electricity price of 0.68 RON per 1 kWh, results in a cost of 3.12 RON per hour. The diesel consumption used for comparison in the internal combustion engine tractor is the lowest, specifically during towing, at a rate of 7.5 liters per hour, and the diesel price at the time of comparison is approximately 7.68 RON per liter. In addition to fuel costs for the internal combustion engine tractor, the following operational costs (estimated costs for one hour of

operation) are added: engine oil - 0.21 RON; hydraulic oil - 2.26 RON; antifreeze - 0.04 RON; oil filter - 0.03 RON; diesel filter - 0.03 RON; total - 2.57 RON.

It can be observed that, in terms of fuel economy, the use of an electric tractor is much more efficient compared to the internal combustion engine tractor.

Chapter 6 Theoretical Research on the Development of Electrically Powered Agricultural Vehicles

Replacing the conventional propulsion system with an electric one in any vehicle, but especially in a tractor, when the chassis remains unaltered, results in a change in mass and consequently a modification in the distribution of forces at the level of the axles and tires. After studying the forces and moments applied at the wheel level, both in static and dynamic conditions, a mathematical model can be created to perform simulations that allow for the study of the behavior of a tractor that has undergone an electric propulsion modification.

6.1. Force and Torque Required for Tractor Movement

The forces applied to the wheels are identical, whether the engine is internal combustion or electric. The forces acting on the tractor are represented in the figure below.

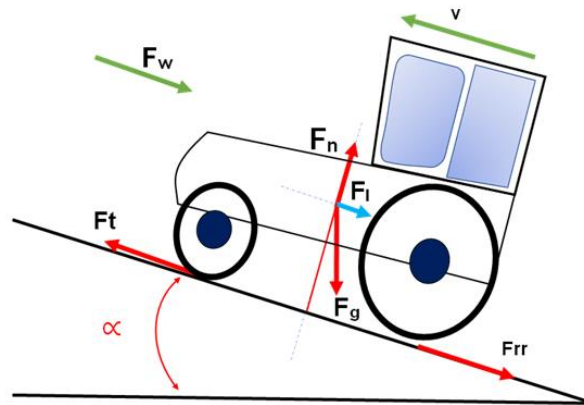


Figure 6.1 Forces acting on the tractor

The traction force of the tractor is calculated with the relation [85]:

$$F_t = F_I + F_{gt} \pm F_{rr} \pm F_w = ma_t + mg \sin \alpha \pm vmg \cos \alpha c_{rr} \pm (v + v_w) \frac{1}{2} \rho C_d A_f (v + v_w)^2 \quad (6.1)$$

$$C_{rr} = 0,001 \left(1 + \frac{3,6}{100} v \right) \quad (6.2)$$

Table 6.1 Various values of the rolling resistance coefficient for specific travel speeds of a tractor calculated using Equation 6.2.

Tractor speed (m/s)	1	5	10	20	50	70	100
Tractor speed (km/h)	3,6	18	36	72	180	252	360
Coefficient of rolling resistance of the wheels, calculated - C_{rr}	0,001	0,001	0,001	0,002	0,003	0,004	0,005

In accordance with the tractor dynamics, Equation 3.143, the engine force can be written as follows:

$$F_m = F_r + F_t \pm F_\alpha + F_a \pm F_j + F_f \quad (6.3)$$

F_j and F_f can be neglected as they have extremely small values in reality. The traction force has been calculated for the following situations:

- Travel on a horizontal plane;
- Travel on an inclined plane.

6.1.1. Case of Travel on a Horizontal Surface

Conditions: $\alpha=0$, resulting in $\sin \alpha$ is 0, the angle γ is 0 so $\text{tg } \gamma$ is 0, $\cos \alpha$ is 1, wind speed is below 1 m/s and is therefore negligible, f is 0,001 and F_α is 0. The travel distance is 50 m, with a speed of 15 km/h (4.16 m/s) for the electric tractor, 13 km/h (3.6 m/s) for the

vegetable electric tractor, 17 km/h (4.7 m/s) for the electric transport tractor, and 10 km/h (2.8 m/s) for the electric vehicle for spraying. The aerodynamic coefficient is that of a cube, considered as $C_d = 1,05$.

Equation (6.3) becomes:

$$F_m = ma_t + mgc_{rr} + v \frac{1}{2} \rho C_d A_f v^2 \quad (6.4)$$

6.1.2. Case of Travel on an Inclined Surface

Conditions: The wind speed is below 1 m/s and is negligible, c_{rr} is 0,001, F_j and F_f are negligible; the slope angle $\alpha = 20^\circ$, $\sin 20^\circ = 0,342$, $\cos 20^\circ = 0,939$, the distance is 50 m, and the tractor speeds range from 10 to 15 km/h. no towed equipment is present.

It can be expressed as:

$$F_m' = ma_t + mg \sin \alpha + vmg \cos \alpha c_{rr} + v \frac{1}{2} \rho C_d A_f v^2 \quad (6.5)$$

The results of the calculations are presented in Table 6.2:

Table 6.2 Forces required for tractor movement on a flat or inclined surface with a 20⁰-degree angle, considering estimated mass.

	m (kg)	a_t (m/s ²)	A_f (m ²)	v (m/s)	ρ (kg/m ³)	$\sin \alpha$	$\cos \alpha$	F_m (N)	F_m' (N)
Electric tractor	2000	0,3461	2,434	4,16	1,225	0,912	0,408	824,53	7592,04
Electric vegetable tractor	1500	0,2592	0,779	3,6	1,225	0,912	0,408	426,88	5494,78
Electric transport tractor	1400	0,4418	0,757	4,7	1,225	0,912	0,408	682,79	5427,02
Electric vehicle for spraying	1300	0,1568	1,682	2,8	1,225	0,912	0,408	240,33	4622,92

Table 6.2 considered an estimated mass of the tractors for the approximate calculation of the driving force that an electric motor must provide for movement.

Table 6.3 The required force for tractor movement when the estimated mass was replaced with the actual mass.

	m (kg)	a_t (m/s ²)	A_f (m ²)	v (m/s)	$\sin \alpha$	$\cos \alpha$	F_m (N)	F_m' (N)
Electric tractor	1970	0,3461	2,434	4,16	0,3420	0,9396	813,859	7479,85
Electric vegetable tractor	1450	0,2592	0,779	3,6	0,3420	0,9396	413,438	5312,39
Electric transport tractor	1379	0,4418	0,757	4,7	0,3420	0,9396	673,315	5346,38
Electric vehicle for spraying	1283	0,1568	1,682	2,8	0,3420	0,9396	237,506	4562,78

6.2. Calculation of the minimum torque required for tractor movement

In order for the tractor to move, it is necessary for the engine force to generate a sufficiently large torque at the wheel level to set the tractor in motion.

According to the equation:

$$T_r = F_m r_m = \frac{M_m}{r_m} = \frac{M_e i_{tr} \eta_{tr}}{r_m} \quad (6.6)$$

It follows that:

$$M_m = F_m r_m \quad (6.7)$$

$$M_e = \frac{F_m r_m}{i_{tr} \eta_{tr}} \quad (6.8)$$

The following table specifies the gear ratios installed in the four electric tractors that were studied.

Table 6.4 Transmission ratios of the transmissions installed in the four agricultural vehicles.

Gear	Total gear ratio					wheel reducer	Total gear ratio speed 1	total gear ratio speed 4
	1	2	3	4	reverse			
Electric tractor	6,18	3,83	2,76	2,09	4,96	2,94	18,17	6,14
Electric vegetable tractor	5,80	3,70	2,90	1,63	4,98	11,38	66,00	18,55
Electric transport tractor	6,01	4,10	3,20	1,52	5,04	10,12	60,82	15,38
Electric vehicle for spraying	4,83	3,54	2,13	1,02	3,80	NA	4,83	3,80

One of the initial calculation hypotheses was that when the engine force is at least equal to the resistance forces, in this case, the engine power must be increased to surpass the inertial forces that occur in the force system.

Considering this hypothesis, acceleration depends on the engine torque. The condition for movement to occur is: $T_r = R_f \leq R_f \text{ lim}$. In this situation, the wheel is in uniform or accelerated motion ($T_r \leq R_f$), the actual torque in electric motors is equal to the torque generated by the motor and depends on the speed.

The required traction torque is calculated using the following relationship, with the condition that the transmission ratio is equal to 1:

$$M_m = F_m r_m \quad (6.9)$$

For the calculation of the minimum power for the movement of the four types of agricultural vehicles at a speed of 10 km/h, the relationship is used:

$$P_m = F_m v \quad (6.10)$$

The minimum electric motor torque required for the movement of agricultural vehicles is:

$$M_g = \frac{M_t}{\eta_m r_m} \quad (6.11)$$

Table 6.5 Moments calculated for the movement of agricultural vehicles on both horizontal and inclined surfaces.

	r_m (m)	i_{tr}	F_m (N)	F_m' (N)	M_e (Nm)	M_e' (Nm)	M_m (Nm)	M_m' (Nm)
Electric tractor	1,05	6,14	813,85	7479,85	169,602	1558,746	854,552	7853,852
Electric vegetable tractor	1,3	18,55	413,43	5312,39	35,335	454,036	537,471	6906,120
Electric transport tractor	1,3	15,38	673,31	5346,38	69,394	551,017	875,311	6950,294
Electric vehicle for spraying	0,88	3,80	237,50	4562,78	67,075	1288,590	209,006	4015,247

The values of torque for the electric motors used in electric tractors are listed in Table 6.6. Since the maximum speed of the electric motor in tractors was limited to 2300 rpm, the values are up to this speed. With knowledge of these values, the actual wheel torque for the first speed stage can be calculated.

So, in conclusion, the main difference lies in the power source: mechanical torque is generated by manually or mechanically applied force, whereas electric torque is generated by the interaction of magnetic fields in an electric motor.

During field tests with the tractor, data provided by the motor controller were recorded, and the results are detailed in Figure 6.2.

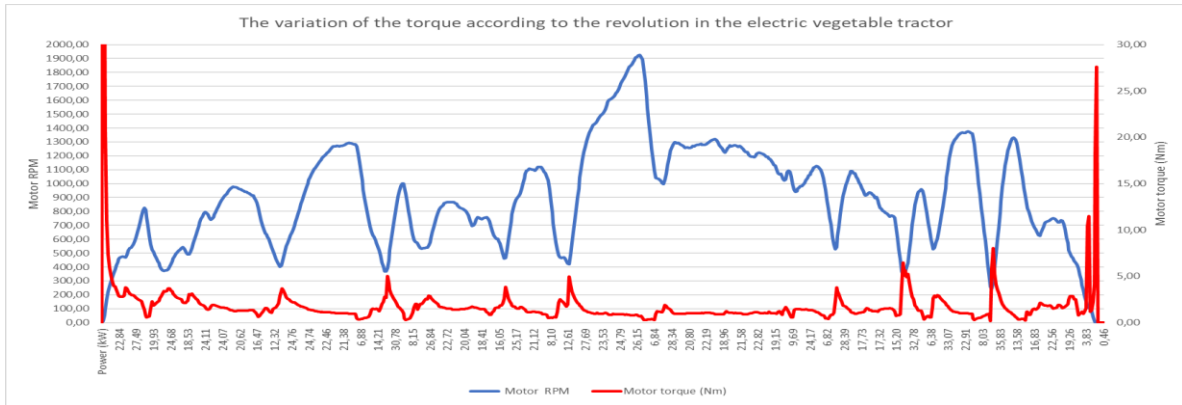


Figure 6.2 The variation of the motor torque according to the speed of the electric vegetable tractor

6.3 Calculation of the required power for the propulsion system

The power at the electric motor shaft is determined by the relationship:

$$P_g = M_g \omega_g \quad (6.12)$$

To calculate the power required for starting from a standstill, the values of the torque generated by the motor at certain speeds were used. The calculated values are presented in Table 6.6.

Table 6.6 Power consumed by electric tractors at different motor speeds.

M_g (Nm)	RPM	ω_g	P_g (W)
Electric tractor			
142	500	52,361	7435,333
139,8	1000	104,723	14640,276
137,8	1500	157,084	21646,245
134,8	2000	209,446	28233,322
134,2	2300	240,862	32323,803
Electric vegetable tractor			
142	500	52,361	7435,333
139,8	1000	104,723	14640,276
137,8	1500	157,084	21646,245
134,8	2000	209,446	28233,322
134,2	2300	240,862	32323,803
The electric vehicle for spraying			
80	500	52,361	4188,920
78,9	1000	104,723	8262,645
77,8	1500	157,084	12221,174
76,1	2000	209,446	15938,841
75,7	2300	240,862	18233,322
Electric transport tractor			
118	500	52,361	6178,657
116,5	1000	104,723	12200,230
114,8	1500	157,084	18033,301
112,3	2000	209,446	23520,787
111	2300	240,862	26735,783

It can be observed that the power required with the smallest value is 4189 W, and the highest power value is 32323 W. These values are only when electric tractors start from a standstill. During movement, these consumptions decrease, and the results are presented in Figure 6.3.

These values are calculated only for vehicle movement on flat surfaces. For movement on inclined surfaces, the power requirement increases. To efficiently use the motor, it must have a higher power rating than the one obtained.

The measured consumption of the electric tractor when starting from a standstill on flat terrain, without a load, in 11.6 seconds is presented in Figure 6.3:

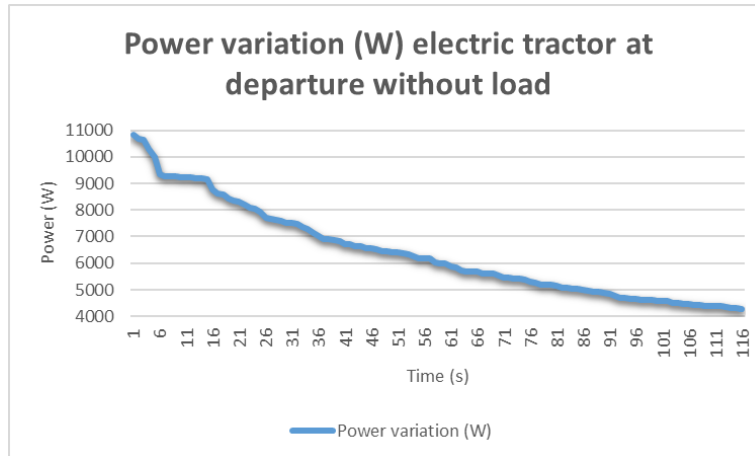


Figure 6.3 Power consumed when the electric tractor starts without load

It is crucial to monitor current variations as the vehicle's efficiency is a function of current.

$$M_m = f(I) \quad (6.13)$$

$$\eta_m = f(I) \quad (6.14)$$

An electric tractor requires an energy surplus, and the battery must provide this surplus without a significant reduction in autonomy. Therefore, when selecting the battery capacity, these consumers must also be considered. An additional estimated consumption is 1320 W, which is added to the motor's consumption.

Figure 6.4 shows the real-time variation of power and speed during movement on an undistorted flat terrain.

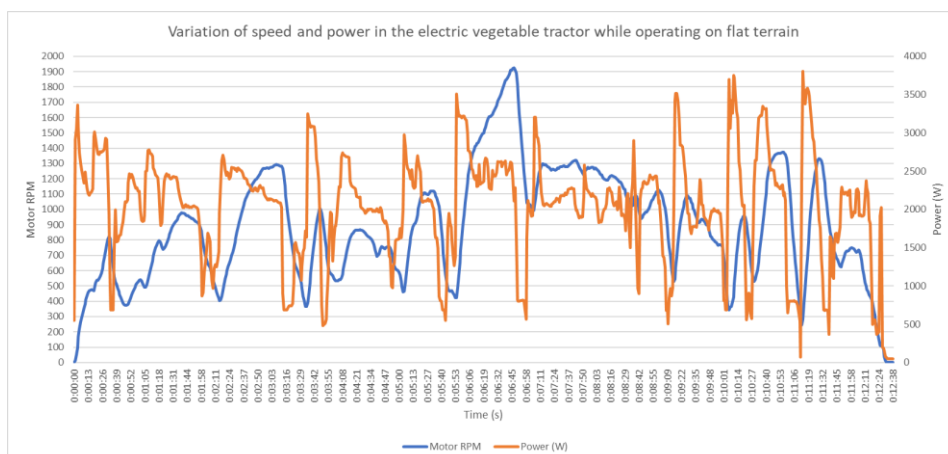


Figure 6.4 Actual variation of power and rpm while driving in the electric vegetable tractor

The batteries have been chosen so that the discharged energy can cover the vehicle's operation for at least 60 minutes at maximum power.

The battery charging system is designed so that it can be powered from the electrical grid available in almost any household, which is a voltage supply of 220 V alternating current with a current ranging from 6 A to 32 A.

Figure 6.5 depicts the charging mode when the charger is supplied with 220 V and 16 A.

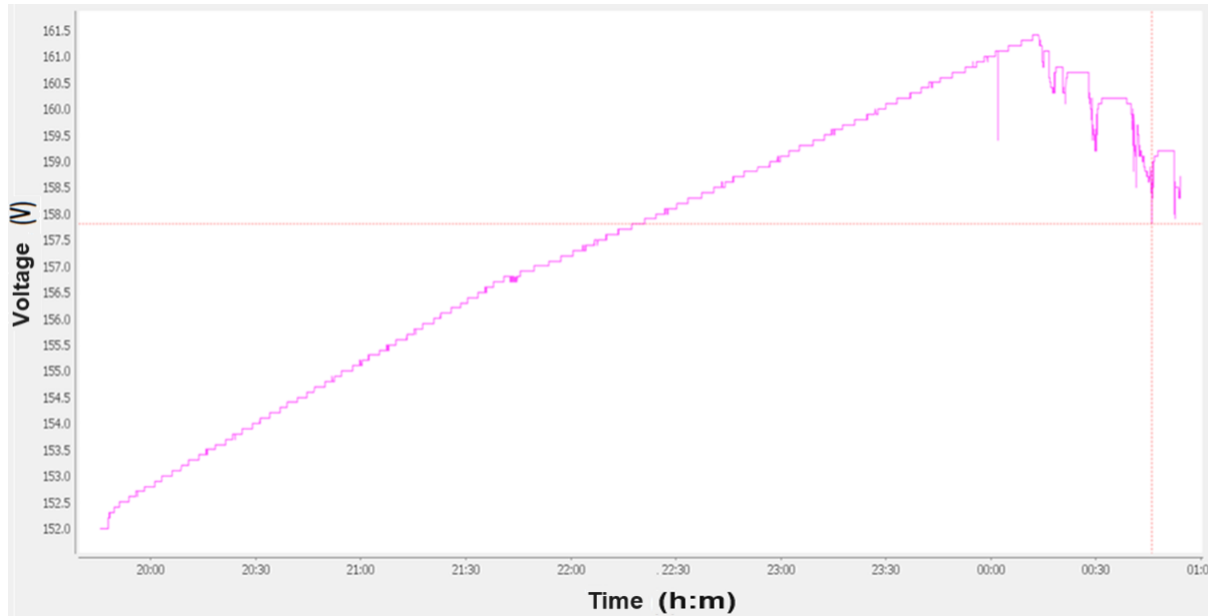


Figure 6.5 Variation of voltage when charging the battery

In figure 6.6 you can see how the voltage on each cell increases in steps.

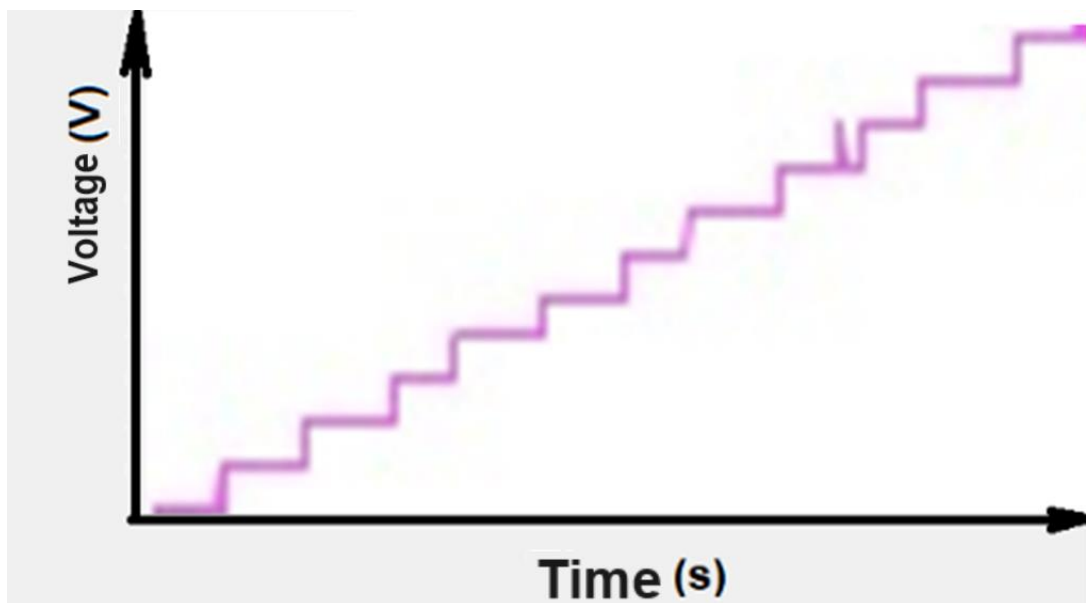


Figure 6.6 Detail with the voltage variation when charging

6.4 Calculation of the center of gravity

Once the types of motors to be used were determined, they were mounted on chassis, and the next step was to weigh the vehicles. The result is presented in Table 6.7:

$$G_t = mg$$

Table 6.7 Real weight of electric agricultural vehicles.

No.	Characteristic	M.U.	The value of the parameters determined in tests
1.	Total weight of electric tractor	N	19325,70
2.	Total weight electric vegetable tractor	N	14224,50
3.	Total weight electric transport tractor	N	13527,99
4.	Total weight of the electric spraying vehicle	N	12586,23

Using relations (3.24, 3.71, 3.72,.3.56) "a" and "b" were calculated to find the position of the center of gravity.

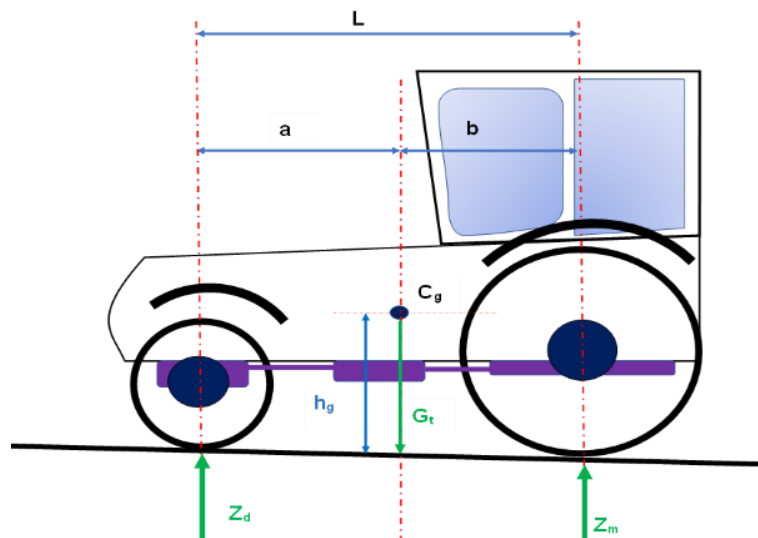


Figure 6.7 Distribution of forces on the vehicle's axles

The following relationships are known: Z_d the normal reaction of the ground on the front axle and is equal to the weight on the front axle [N]; Z_m is the normal reaction of the ground on the rear axle and is equal to the weight on the rear axle [N]; L - wheelbase [m]; m_f - mass on the front axle [kg]; m_s - mass on the rear axle [kg]; G_t - total weight [N];

We have the following relationships:

$$a = \frac{Z_m L}{G_t} \quad (6.15)$$

$$b = \frac{Z_d L}{G_t} \quad (6.16)$$

Table 6.7 The position of the center of gravity is relative to the front and rear axles.

	L (m)	Z_d (N)	Z_m (N)	a (m)	b (m)	G_t (N)
Electric tractor	2,02	7357,5	11968,2	1,25	0,77	19325,70
Electric vegetable tractor	2,3	5052,15	9172,35	1,48	0,82	14224,50
Electric transport tractor	2,3	4797,09	8730,9	1,490	0,81	13527,99
Electric spraying vehicle	2,7	4718,61	7867,62	1,690	1,01	12586,23

Figure 6.8 shows the weight distribution on the front/rear axles of the electric vehicles used in the experiments.

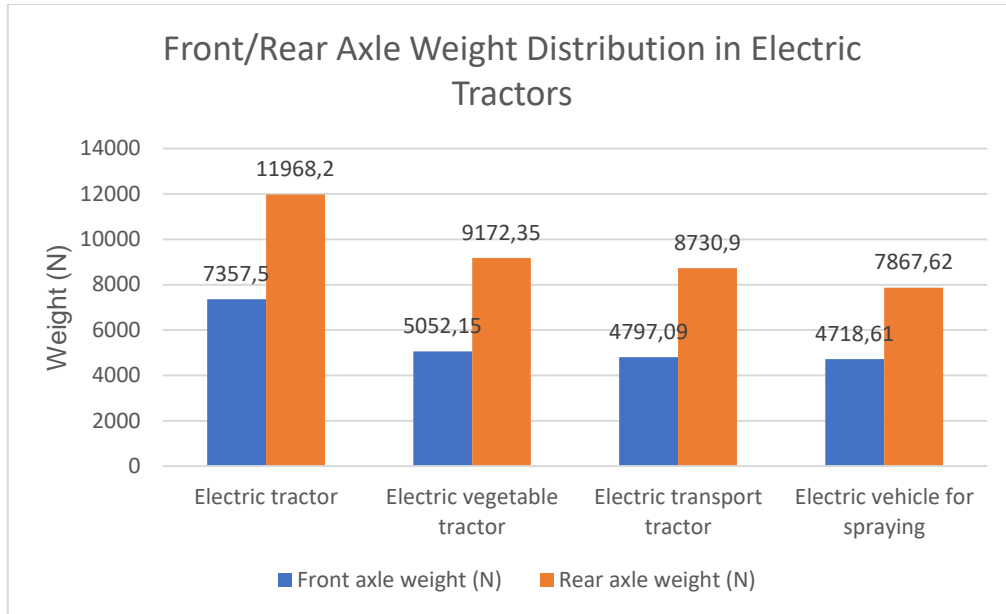


Figure 6.8 The difference in weight on the axles of the electric vehicles used in the experiments

6.5. Changing the position of the center of gravity

In the experiments and studies conducted, it was found that the rolling resistance coefficient is influenced by a multitude of factors:

- Travel speed;
- Tire pressure;
- Wheel load;
- Applied wheel torque;
- Tread surface;

Table 6.9 presents the values used in calculations of the rolling resistance coefficient (f) as defined by equation (3.91).

Table 6.8 Average values of the rolling resistance coefficient. [37]

The running surface	Rolling resistance coefficient
Asphalt or concrete	0,015-0,020
River gravel road	0,025-0,050
Broken stone road	0,020-0,025
Beaten dirt road	0,025-0,250
Sandy dirt road	0,040-0,300
Stubble	0,100-0,120
Meadow	0,07-0,100
Freshly plowed field	0,180-0,220
Cultivated field	0,160-0,250

In equation (3.49), the coefficient of adhesion and the coefficient of utilization of adhesion are defined, while the slip ratio is defined in equation (3.48).

As a result:

$$v_r = v_t(1 - \delta) \quad (6.17)$$

The compressive effort on the track is:

$$\sigma = CD_{cr}^n \quad (6.18)$$

Experimental values for "C" have been determined:

$$C = \frac{\sigma}{y^n} \tag{6.19}$$

Table 6.9 Values from the specialized literature of the coefficient C, which depends on the deformation of the track. [37]

Tread surface	C value
Understandable soil	9...20
Cultivated soil	15
Earth	9...12
Sand	3...5

A coefficient that depends on the traction force and the wheel load, called the coefficient of utilization of adhesion weight, φ_{ga} , can be defined. Thus, we have the relationship: [37]:

$$\varphi_{ga} = \frac{F_t}{G_{ad}} \tag{6.20}$$

$$G_{ad} = \frac{Q_c}{2} \tag{6.21}$$

Table 6.11 calculates the coefficient of utilization of adhesion weight for vehicles equipped with electric propulsion systems in the first speed stage.

Table 6.10 Values of the coefficient of utilization of adhesion weight.

	φ_{ga}	G_{ad} (N)	Q_c (N)
Electric tractor	0,136004	5984,10	11968,20
Electric vegetable tractor	0,090149	4586,18	9172,35
Electric transport tractor	0,154237	4365,45	8730,90
Electric vehicle for spraying	0,060376	3933,81	7867,62

Figures 6.9, 6.10, and 6.11 depict the wheel loads for each electric tractor (Q_c) and the values of the coefficient of utilization of wheel weight (φ_{ga}). These loads and the coefficient of utilization of weight are calculated for flat terrain.

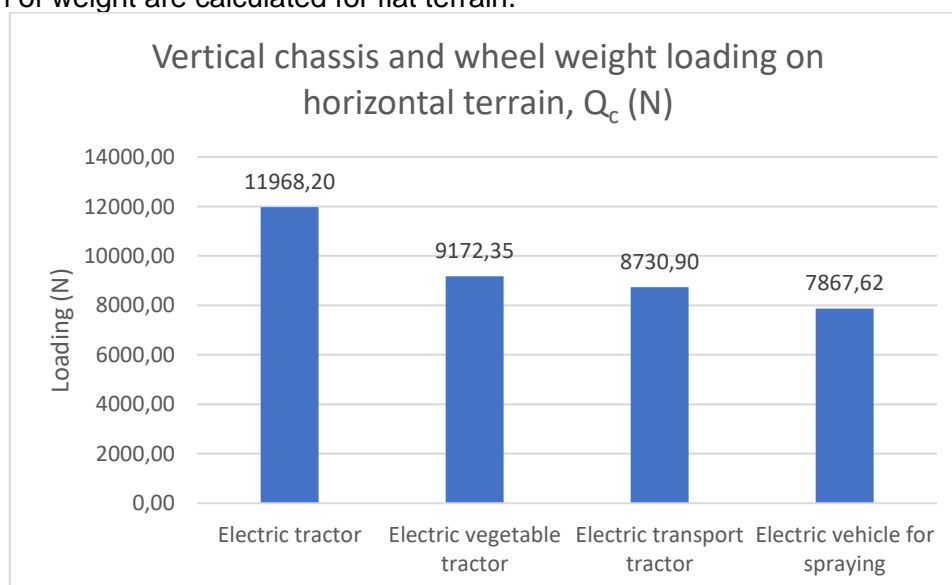


Figure 6.9 The graph with the values of the vertical load in electric tractors

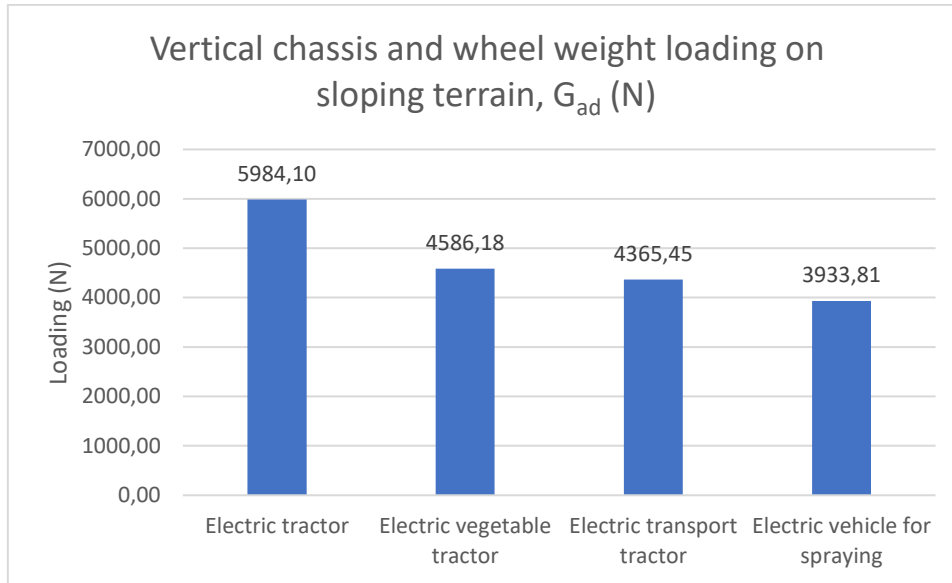


Figure 6.10 The graph with the values of the vertical load on the sloping terrain of electric tractors

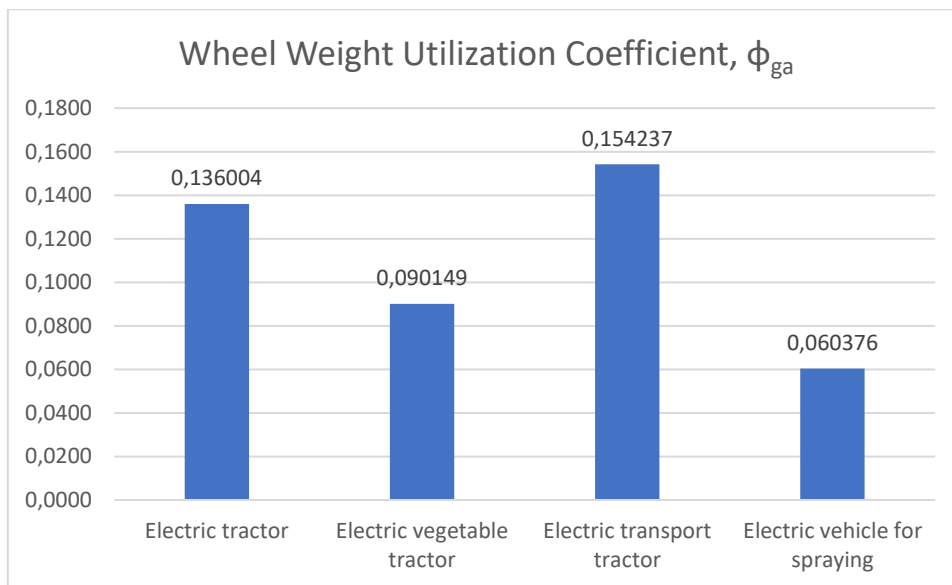


Figure 6.11 The graph with the coefficient of use of the weight on the wheel for electric tractors

If the mass is modified by 50 kg (490.3325 N) and 75 kg (735.49875), there is a change in the coefficient of utilization of weight, as shown in Table 6.12.

Table 6.11 Modification of the coefficient of utilization of weight.

	Φ_{ga}	Φ'_{ga}	Φ''_{ga}	Q_c' (N)	Q_c'' (N)
Electric tractor	0,1360035	0,1257	0,121117192	6474,43	6719,60
Electric vegetable tractor	0,0901489	0,0814	0,077689617	5076,51	5321,68
Electric transport tractor	0,1542374	0,1387	0,13199815	4855,78	5100,95
Electric vehicle for spraying	0,0603757	0,0537	0,050865525	4424,14	4669,31

Figure 6.12 shows the graph depicting changes in the weight utilization coefficient as the weight on the tractor axles is altered, resulting in a change in wheel load.

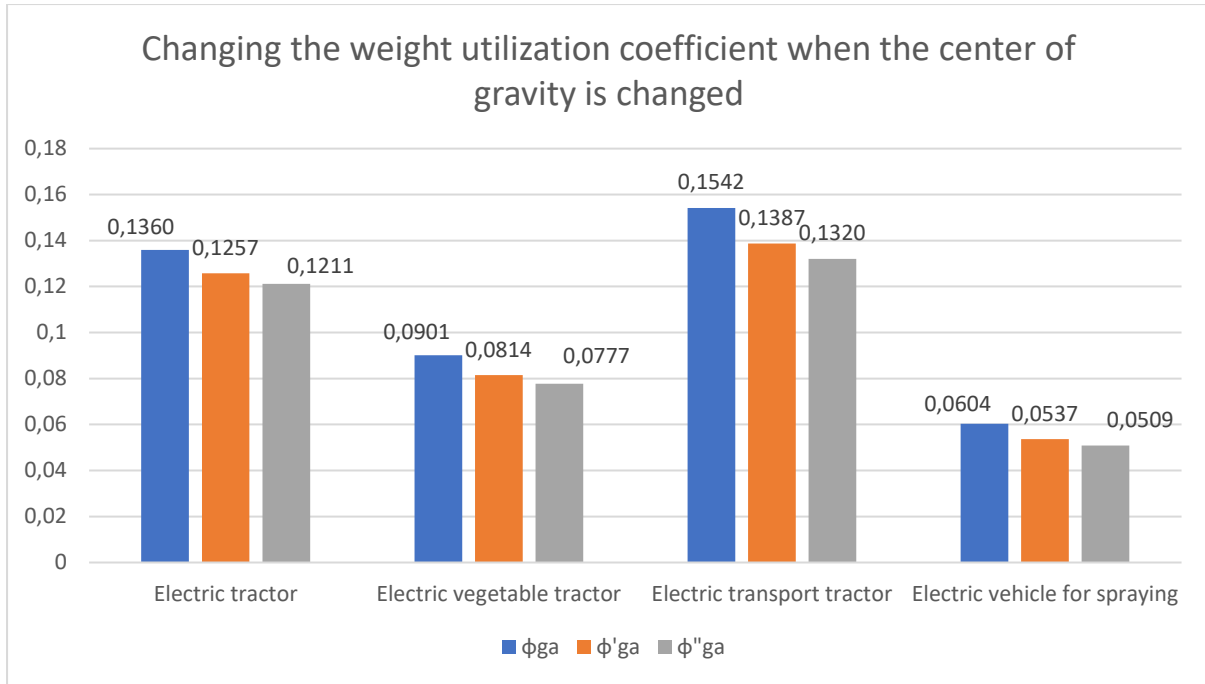


Figure 6.12 Variation of weight utilization coefficient when center of gravity is changed

Figure 6.13 shows the change in weight on the wheel when additional weight is added to the tractor.

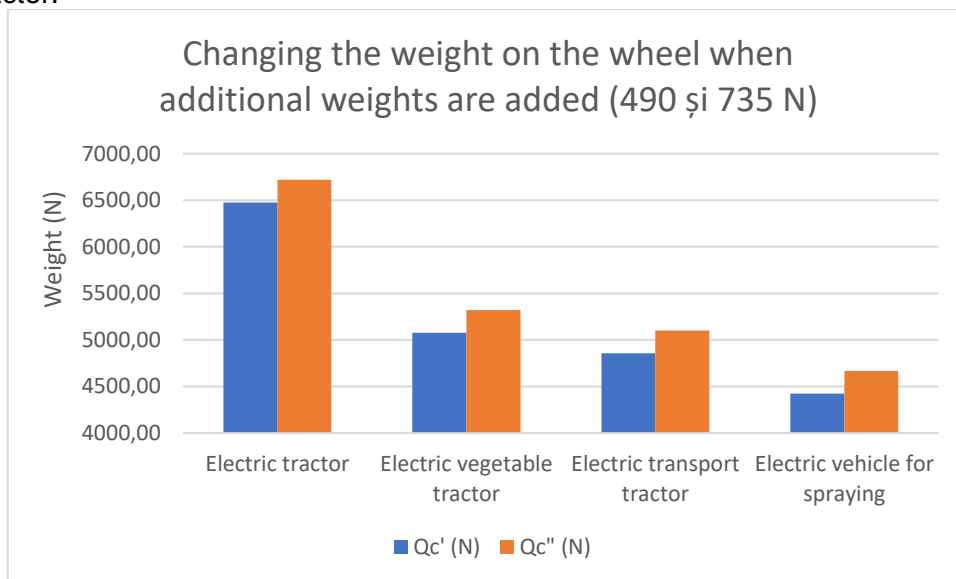


Figure 6.13 Changing the weight on the wheel when additional weights are added

It can be observed that the traction force depends on the coefficient of friction, the tread surface, and the load acting on the wheel. Since the only variable that can be controlled is the wheel load, a mobile support was created on which the battery and the entire electronic propulsion control system were mounted so that the position of the center of gravity can be modified, within certain limits, allowing the forces acting on the wheels to be adjusted.

The slip ratio is calculated with the equation [37]:

$$\delta = a_a \frac{F_t}{G_{ad}} + b_b \left(\frac{F_t}{G_{ad}} \right)^{c_c} \quad (6.22)$$

The coefficients, a_a , b_b and c_c , in equation (6.22) are influenced by variables such as the type of tire used, tire air pressure, and the nature of the ground the tractor is moving on.

Table 6.13 presents the calculated values of the wheel slip coefficient for vehicles used in the experiments, on flat terrain and in the 1st speed stage, with tire pressures of 0.7 and 1.0 bar (7 and 10 N/cm²).

Table 6.12 Calculated values of the wheel slip coefficient.

Soil condition/Tyre pressure	Electric tractor	Electric vegetable tractor	Electric transport tractor	Electric vehicle for spraying
δ for loose soil/ 7 N/cm ² (%)	1,632600	1,081835	1,852034	0,724514
δ for compact soil/ 7 N/cm ² (%)	1,360046	0,901490	1,542404	0,603758
δ for loose soil/ 10 N/cm ² (%)	1,632910	1,081861	1,852694	0,724516
δ for compact soil/ 10 N/cm ² (%)	1,360051	0,901490	1,542415	0,603758

The traction force that must be generated by the tractor at the wheel depends on the ground friction with the tire and the weight distributed at the wheel, and it can be calculated using the following relationship:

$$F_{tm} = \eta Q_{mm} + \sigma A c \tag{6.23}$$

In the calculation of the traction force, the product of the compressive effort and the total area of the contact surface with the ground is denoted as "Q". The results are presented in the table below.

Table 6.13 Calculated values of the traction force.

	F _{tm} (N)	η	Q _{mm} (N)
Electric tractor	2250,0216	0,7520	2992,0500
Electric vegetable tractor	1724,4018	0,7520	2293,0875
Electric transport tractor	1641,4092	0,7520	2182,7250
Electric vehicle for spraying	1479,1126	0,7520	1966,9050

Moving the position of the center of gravity forward or backward can reduce wheel slip for certain types of work or terrains. This can be achieved without adding additional weights to the tractor but by adjusting the position of the battery and electronic equipment, which are mounted on a frame that can be positioned at different distances from the tractor's axles.

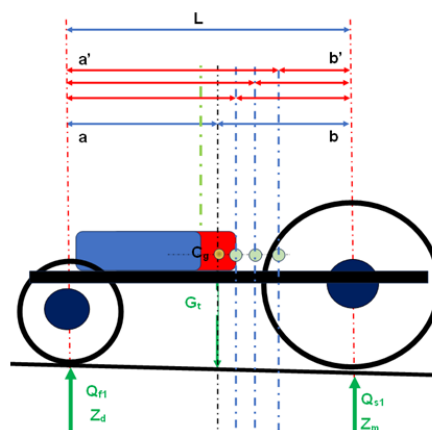


Figure 6.14 Changing the center of gravity position when the battery is moved to the rear axle

Changing the working position of the battery, due to the construction, is only possible with the electric tractor. After the battery position was modified towards the rear by 5, 10, 15, and 20 cm (Figure 6.14), replacing the new values of "a" and "b" (the distances from the center of gravity to the front/rear axles - Figure 6.8) in equations 6.14 and 6.15, the following values for the weights on the front and rear axles are obtained.

Table 6.14 Presents the values obtained through calculations for the weights distributed on the electric tractor's axles and the distances from the center of gravity to the front and rear axles when the battery is moved to the rear.

	L (m)	Q_{r1} (N)	Q_{s1} (N)	a' (m)	b' (m)	G_t (N)	Changing the position (m)
Electric tractor	2,02	6879,141	12437,33	1,30	0,72	19325,7	0,05
Electric tractor	2,02	6400,782	12924,92	1,35	0,67	19325,7	0,10
Electric tractor	2,02	5922,423	13403,28	1,40	0,62	19325,7	0,15
Electric tractor	2,02	5444,064	13881,64	1,45	0,57	19325,7	0,20

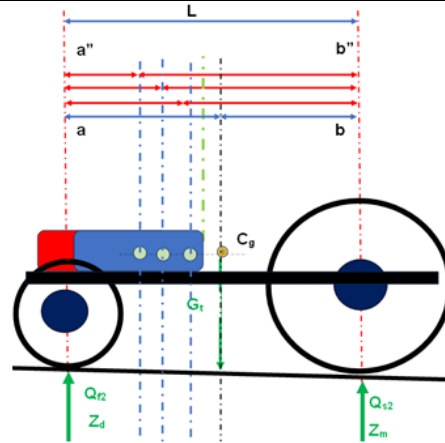


Figure 6.15 Changing the center of gravity position when the battery is moved to the front axle

The following table presents the variation of the weights on the electric tractor's axles when the battery is moved 5, 10, 15, and 20 cm forward from the initial mounting point.

Table 6.15 Displays the values obtained through calculations for the weights distributed on the electric tractor's axles and the distances from the center of gravity to the front and rear axles when the battery is moved to the front.

	L (m)	Q_{f2} (N)	Q_{s2} (N)	a'' (m)	b'' (m)	G_t (N)	Changing the position (m)
Electric tractor	2,02	7835,859	11489,84	1,20	0,82	19325,7	0,05
Electric tractor	2,02	8314,218	11011,48	1,15	0,87	19325,7	0,10
Electric tractor	2,02	8792,577	10533,12	1,10	0,92	19325,7	0,15
Electric tractor	2,02	9270,936	10054,76	1,05	0,97	19325,7	0,20

Figure 6.16 shows the variations in the weights on the front and rear axles when the battery is moved 5, 10, 15, and 20 cm forward and backward from the initial point.

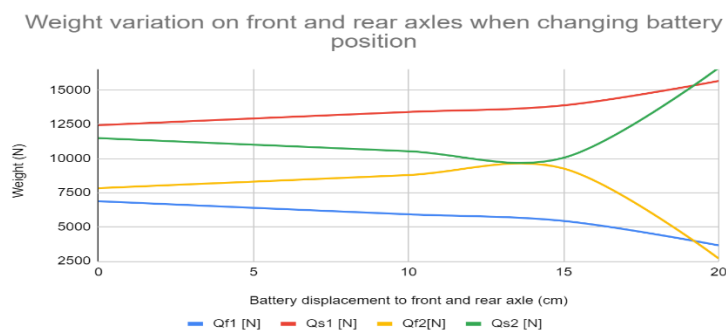


Figure 6.16 Weight variation on the front and rear axle when changing the battery position

6.6. Total efficiency

As described in equation (3.11), the total efficiency is the product of the efficiencies of all the subassemblies that make up the transmission. When some of the subassemblies composing the transmission are eliminated, for example, the mechanical torque transformer, then equation (3.11) becomes:

$$\eta = \eta_m \eta_{tr} \quad (6.24)$$

The efficiency of a three-phase synchronous motor with permanent magnets ranges from 95% to 98%. The lower value will be considered.

$$\eta_m = 0,95 * 0,86 = 0,82 \quad (6.25)$$

Figure 6.17 presents a graph showing the efficiency difference between internal combustion engines and electric motors, a general graph used for comparison purposes only.

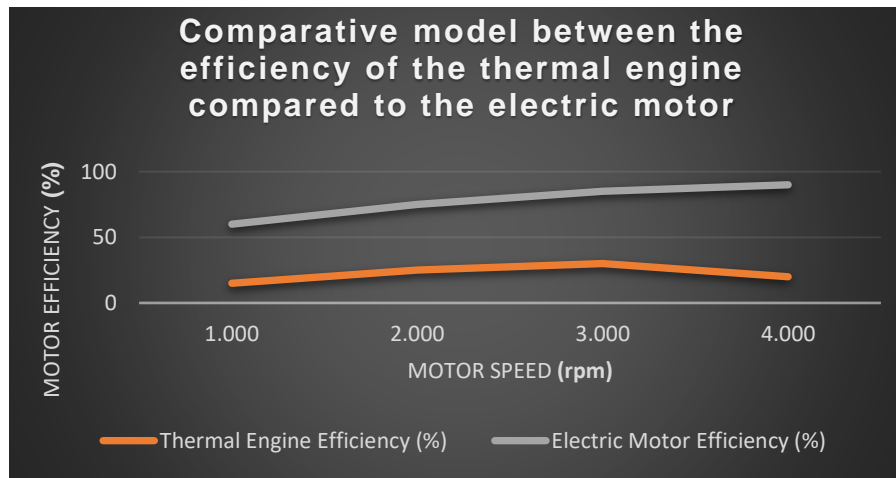


Figure 6.17 Comparison between the efficiency (in general) of the heat engine and the electric engine

Simplified efficiency is defined as:

$$\eta_m = \frac{P_a}{P_{b-out}} [\%] \quad (6.26)$$

For electric vehicles, the power generated during regenerative braking [85] is given by

$$P_{b-in} = \frac{\psi v}{\eta_t \eta_m} \left(M_v g (f_r + i) + \frac{1}{2} \rho_a C_D A_f v^2 + M \delta \frac{dv}{dt} \right) \quad (6.27)$$

The total actual energy consumed from the battery is calculated as:

$$E_{out} = \int_{tracțiune} P_{b-out} dt + \int_{frână} P_{b-in} dt \quad (6.28)$$

However, in the case of a tractor, there is no energy generated by the motor, so $P_{b-in} = 0$.

6.7. Rotor Slip

The variation of the torque-speed relationship of the motor can be controlled by modifying the voltage applied to the motor terminals and the frequency of this voltage. When calculating the motor speed, consideration is given to rotor slip, which is determined by the three-phase power supply.

This phenomenon, well-known from previous research on electric vehicles, is used when electric motors, which offer superior control capabilities, are employed. A special processor dedicated to reducing slip can be introduced into the motor control system. This processor determines when slip occurs and applies corresponding corrections to the motor power control. This prevents the loss of control or, in other words, keeps the tractor's maneuverability within specified limits, while also reducing energy consumption.

Manufacturers of electric motor controllers have additionally incorporated a specialized circuit into the operation diagram, which is tasked with reducing or even eliminating the slip effect that occurs in electric motors.

6.8. Energy Consumption

Battery capacity is measured in kWh; therefore, autonomy can be relatively easily calculated. The relationship expressing the energy consumed from the battery, without auxiliary consumers, is as follows:

$$P_{b-out} = \frac{v}{\eta_t \eta_m} \left(M_v g (f_c + i) + \frac{1}{2} \rho_a C_D A_f v^2 + M \delta \frac{dv}{dt} \right) \quad (6.29)$$

The estimated calculation of energy consumed from the battery for all four agricultural vehicles on flat terrain is provided. The slope angle is zero, $\rho = 1.225 \text{ kg/m}^3$, $\sin \alpha = 0$, $C_D = 1,05$, $g = 9,81$, $f_r = 0,001$, δ estimated at $0,0026$, $\eta_m = 0,95$, $\eta_t = 0,86$.

Table 6.16 Estimated energy consumed from the battery for 15 seconds.

	time (s)	A_f (m ²)	v (m/s)	η_t	η_m	P_{b-out}
Electric tractor	15	2,434	4,16	0,86	0,95	236,337
Electric vegetable tractor	15	0,779	3,6	0,86	0,95	91,2884
Electric transport tractor	15	0,757	4,7	0,86	0,95	139,691
Electric vehicle for spraying	15	1,682	2,8	0,86	0,95	72,2004

The energy consumed from the battery is not only the one used by the motor. The propulsion system's auxiliary systems are powered even when the vehicle is not moving, with an average consumption of about 800W.

With the help of the BMS (Battery Management System), a report on the energy consumption from the battery was generated, and the recorded values are presented in Table 6.18.

Table 6.17 Shows the measured energy consumed from the battery in the electric tractor for a duration of 15 seconds.

Time (s)	Battery current (A)	Battery voltage (V)	Battery power (W)
00:00:00	1,4	163,1	228,34
00:00:01	1,4	163,1	228,34
00:00:02	1,4	163,1	228,34
00:00:03	2,8	163	456,4
00:00:04	6,4	162,9	1042,56
00:00:05	10,3	162,7	1675,81
00:00:06	16	162,5	2600
00:00:07	14,1	162,5	2291,25
00:00:08	7,6	162,8	1237,28
00:00:09	15,8	162,5	2567,5
00:00:10	7,1	162,8	1155,88
00:00:11	6,1	162,8	993,08
00:00:12	10,4	162,7	1692,08
00:00:13	7,9	162,7	1285,33
00:00:14	9,1	162,7	1480,57
Average power (W)			1360,38

There is a difference between the estimated energy and the actual energy.

The graph depicting the voltage and current variation over 15 seconds for the electric transport tractor is presented in Figure 6.18.

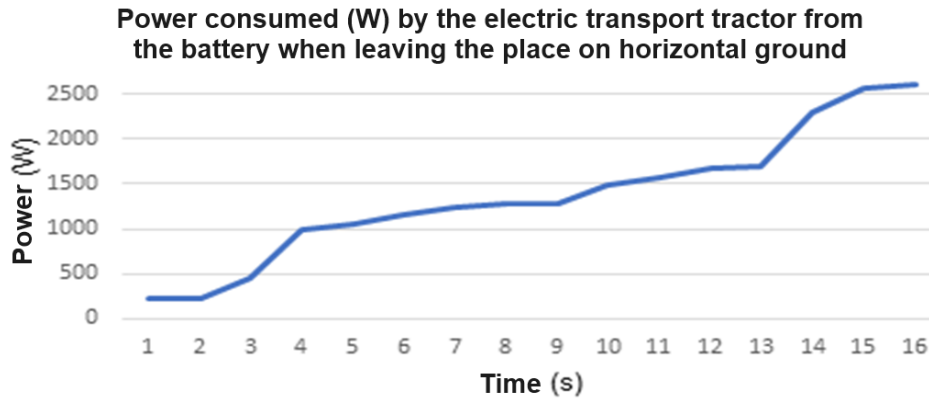


Figure 6.18 Energy consumption from the battery for 15 seconds in the electric tractor

The estimated calculation of energy consumed from the battery for all four agricultural vehicles, moving on a 10-degree inclined terrain (0.1745 rad), with the remaining conditions being the same as mentioned earlier.

Table 6.18 Displays the power consumed during a 15-second journey.

	Time (s)	m (Kg)	A _f (m ²)	V (m/s)	η_t	η_m	P _{b-out}
Electric tractor	15	1970	2,434	4,16	0,86	0,95	17323,8
Electric vegetable tractor	15	1450	0,779	3,6	0,86	0,95	10975,3
Electric transport tractor	15	1379	0,757	4,7	0,86	0,95	13653,6
Electric spraying vehicle	15	1283	1,682	2,8	0,86	0,95	7562,55

Tests were conducted over a longer duration, with the vehicles being used under different loads, then recharged and used again.

In Figure 6.19, a report generated by the propulsion system's BMS is presented, covering the use of the electric tractor for approximately 6 hours.

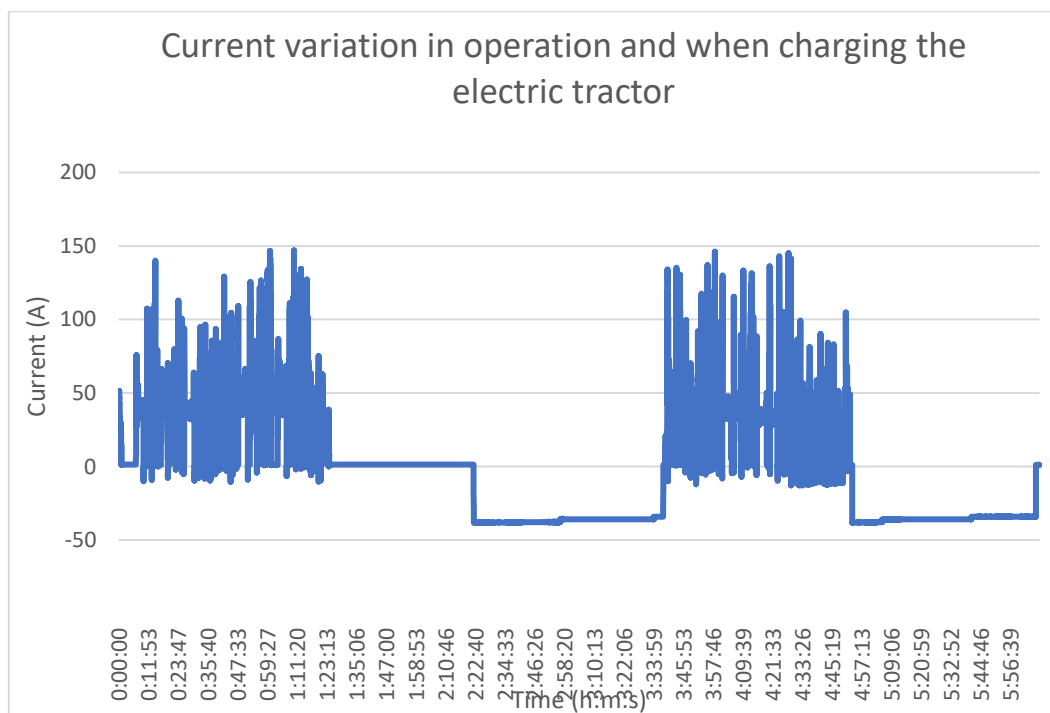


Figure 6.19 Consumption from the battery of the electric tractor for 6 hours

When analyzing tables with many rows and columns, such as the file that generated the graph in Figure 6.20, Python 3.8.10 can be utilized along with the "pandas" and "datetime" libraries.

6.9. Battery charging

Charging time is an important parameter when discussing an electric vehicle. Battery charging is done from the electric power supply network. Outlets with a voltage of 220 V at 50 Hz can be used, with a current ranging from 6 A to 32 A.

The calculation relationship for the battery charging time is:

$$T_{inc} = \frac{C_{bat}}{C_{inc}} \tag{6.30}$$

The current required for charging is:

$$C_{inc} = C_{bat} 10\% \tag{6.31}$$

Experiments conducted during battery charging involved different power levels from the electrical outlet, starting from 6 A up to 32 A with 220 V.

Figure 6.20 shows the variation of voltage and current during battery charging. It is worth noting that the current value is represented with negative values, indicating the current with which the charger supplies the battery.

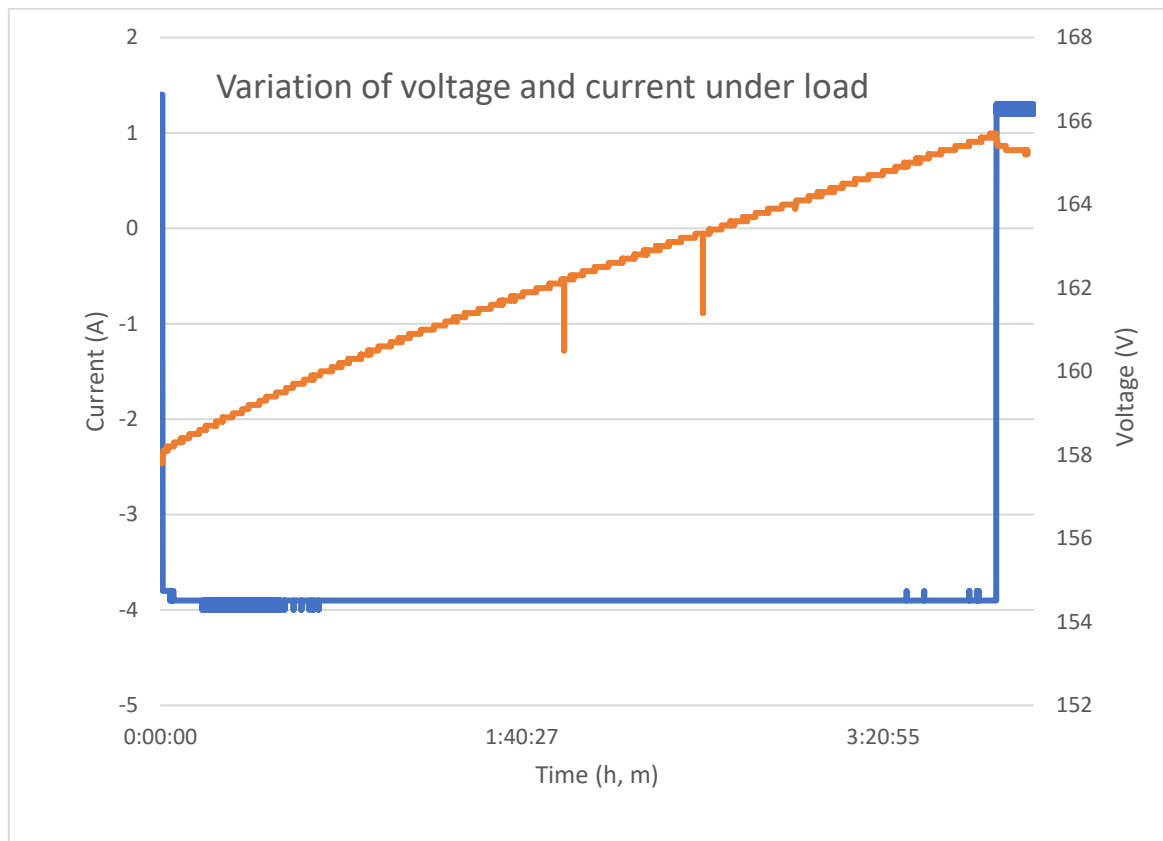


Figure 6.20 Variation of voltage and current under load

When the energy level reaches the one set in the BMS parameters, the charging is interrupted.

Chapter 7 General conclusions, contributions, perspectives

7.1. Conclusions

- ❖ Electric propulsion equipment systems allow adaptation to any type of vehicle.
- ❖ Numerical modeling of a vehicle with electric propulsion involves solving equations whose solutions are implemented on the vehicle in a predefined manner during the design process. Modeling is used to optimize the equipment design. Vehicle acceleration modeling is likely the most typical performance characteristic. Modeling software, such as Excel or Matlab, can provide viable results comparable to real data, and the mathematical model allows the designer to test the characteristics of various subassemblies to find the appropriate equipment for the vehicle, without actual costs. The modeling result can only be validated with real values after the vehicle has been equipped.
- ❖ The study of the electric power supply system for vehicles, according to the charge/discharge graphs and real-world behavior, revealed that the battery behaves within normal limits compared to the results obtained by other electric tractor developers. Charging up to 90% of total capacity took 3 hours, which falls within the average charging time of other similar equipment. The average working time with a load was approximately 4 hours, which is typical for this type of equipment.
- ❖ Electric tractors have significant advantages, especially in enclosed spaces. In enclosed spaces such as greenhouses or solariums, charging stations can be installed with power supply from the national grid or renewable sources, allowing the equipment to be used more efficiently during idle times. If the tractor is used in open fields, it's even possible to bring mobile charging stations closer to where the equipment is used to harness solar or wind energy for battery charging.
- ❖ Using electric propulsion tractors eliminates harmful gas emissions into the atmosphere and has a reduced impact on the soil. This is also due to the fact that when the equipment is powered by electricity from a battery, there is no risk of fossil fuel leaks that could end up on the work surface due to accidents or mishaps.
- ❖ The use of batteries that can be quickly mounted in various positions allows for the adjustment of the tractor's center of gravity as needed, ensuring better traction and easier maneuvering. The ability to change the battery's position results in at least a 15% reduction in slippage compared to a traditional engine tractor.
- ❖ This work demonstrated that electric tractors are more cost-effective over the long term. Currently, producing, integrating, and using electricity as a fuel source may seem expensive and inefficient financially, but long-term calculations show that this technology will bring significant financial and environmental benefits.
- ❖ After all the tests have been conducted, it can be considered that both a vegetable chassis and a general-purpose tractor chassis can be electrically powered by batteries. The tested battery successfully completed the tasks proposed under conditions close to normal.

7.2. Personal contributions

- Bibliographic study on the evolution of tractors in terms of pollution reduction and fuel or energy consumption.
- Bibliographic study on existing engines and transmissions in tractors.
- Bibliographic study of electric propulsion systems in vehicles, especially automobiles.
- Bibliographic study of programs used for configuring and controlling electric propulsion systems.
- Bibliographic study of vehicle dynamics, especially agricultural ones.

- Analysis of the phenomenon of wheel slip in several types of soil for tractors.
- Analysis of the effects of forces and moments on the wheels of 4X2 and 4x4 tractors.
- Analysis of electric propulsion systems mounted on electric vehicles.
- Analysis of the types of errors that may occur during the operation of the electronic control and command systems that make up the electric propulsion system.
- Development of a simulator stand to test the propulsion system before mounting it on the chassis at INMA Bucharest.
- Experimental determination of characteristics for propulsion systems composed of three types of batteries, four types of electric motors, and four types of motor controllers.
- Determination of charging times for the three types of batteries with four types of chargers.
- Participation in the development of four types of supports for fixing electric motors to the chassis used in the experiments.
- Participation in the development of a motor-to-transmission sliding mounting system, for which a patent application was filed with OSIM under registration number A/000648 on October 21, 2021.
- Participation in the development of the first functional Romanian electric tractor at INMA Bucharest.
- Participation in the development of the first fully electric vehicle for spraying at INMA Bucharest.
- Development of a model demonstrating how using the battery as a weight can reduce slippage and improve vehicle maneuverability.
- Demonstration of energy consumption reduction using algorithms optimized for each specific case.;

7.3. Perspectives

This work opens a new horizon for the use of electrical energy in agriculture, especially for tractors, where it was considered unlikely to be powered by electric motors. The paper brings to the attention of agricultural vehicle manufacturers the possibility of using electric propulsion, the advantages of this technology, and the solutions that underlie the further development of these types of vehicles. Additionally, these results can be used by battery developers to achieve enhanced performance specific to such vehicles. Environmental protection researchers can utilize these vehicles to develop new pollution standards.

List of works

1. **Cristea M.**, Matache M., Grigore A.I., Grigore I., Vlăduțoiu L., Persu C., Dumitru I. 2019,- *Study on the use of automotive battery pack for driving agricultural vehicles*, ISB-INMA TEH Volume Symposium pag. 100-108, http://isbinmateh.inma.ro/pdf/Volume_Symposium_2019.pdf;
2. **Cristea M.**, Matache M., Sorică C., Biriș S. Șt., Ungureanu N., Cristea R.D., 2020, *Study on the behavior of a battery mounted on an electric tractor prototype*, INMATEH vol. 62, nr. 3, pag 19-28,
3. **Cristea M.**, Matache M., Sorică C., Grigore A.I., Vlăduțoiu L., Grigore I., Sorică E., Dumitru I., Cristea R.D., 2020, *Study regarding the noise level generated by an electric powered agricultural vehicle*, ISB-INMA-TEH International Symposium, pag. 734-738, https://isbinmateh.inma.ro/wp-content/uploads/2023/02/Volume_Symposium_2020.pdf ;
4. Tudor E., Matache M.G., Sburlan I.C., Vasile I., **Cristea M.**, 2020, *Electric circuits dimensioning for small power electric tractor*, ISB-INMA-TEH International Symposium, pag 104-113, https://isbinmateh.inma.ro/wp-content/uploads/2023/02/Volume_Symposium_2020.pdf ;
5. Nenciu F., Matache M.G., **Cristea M.**, Găgeanu I., Voicea I., 2020, *Research on the use of photovoltaic systems to power off-road electric tractors*, ISB-INMA-TEH

- International Symposium, pag 586-591, https://isbinmateh.inma.ro/wp-content/uploads/2023/02/Volume_Symposium_2020.pdf ;
6. Matache A., Matache M.G., Petre A.A., Vanghele N.A., **Cristea M.**, 2020. *Pollution of the environment and organisms in the context of modern agriculture*, ISB INMA TEH' 2020 International Symposium, Bucharest, pp.515-522, https://isbinmateh.inma.ro/wp-content/uploads/2023/02/Volume_Symposium_2020.pdf ;
 7. Matache M.G., **Cristea M.**, Găgeanu I., Zapciu A., Tudor E., Carpus E., Popa L.D., 2020. *Small power electric tractor performance during ploughing works*, INMATEH Agricultural Engineering, vol 60, nr 1/2020, pp 123-128, <https://doi.org/10.35633/inmateh-60-14> ,
 8. Grigore A. I., Vlăduțoiu L., Sorică C., **Cristea M.**, Petre A.A., Sorica E., 2021, *Aspects regarding the evolution of organic agriculture in Romania and worldwide*, ISB-INMA-TEH International Symposium, pag 668-673, https://isbinmateh.inma.ro/wp-content/uploads/2023/02/Volume_Symposium_2021.pdf ;
 9. **Cristea M.**, Vlăduțoiu L., Grigore A. I., Cristea D. R., 2021, *Types of electric motor controllers that can be used on agricultural electric tractors*, Analele Universității din Craiova, vol. 51;
 10. Tudor E., Matache M. G., Sburlan. I. C., Vasile I., **Cristea M.** 2021. *Experimental validation of combined trip estimator for small power electric tractor*. INMATEH-Agricultural Engineering, vol 64, nr. 2. WOS:000709094600009, <https://inmateh.eu/volumes/volume-64--no-2--2021/experimental-validation-of-combined-trip-estimator-for-small-power-electric-tractor/> ;
 11. **Cristea M.**, Matache, M. G., Ioniță C., Perișoară L. A., Cristea R. D., Arsenoia V. N. 2022. *GSM Wi-Fi mobile communication system for agricultural vehicles*. INMATEH-Agricultural Engineering, vol. 67, nr. 2. WOS:000844838300002, <https://inmateh.eu/volumes/volume-67--no-2--2022/gsm-wifi-mobile-communication-system-for-agricultural-vehicles/> ;
 12. Vasile I.; Tudor E.; Sburlan I.-C.; Matache M. G.; **Cristea M.** 2023. *Optimization of the Electronic Control Unit of Electric-Powered Agricultural Vehicles*. World Electr. Veh. J. 2023, 14, 267. <https://doi.org/10.3390/wevj14100267>. <https://www.mdpi.com/2032-6653/14/10/267> ;
 13. **Cristea M.**, Biriș S. Șt., Cristea R.D., Tăbărașu A., 2023, *The use of electric motors for the propulsion of agricultural vehicles*, Universitatea Politehnica București Buletin Științific article being evaluated.

Patent application

1. Ciupercă Radu, Matache Mihai, Zaica Ana, Persu Cătălin, **Cristea Mario**, 2012, *Innovative technical system for assembling electric motors on electrically driven agricultural machines*, nr. request A-00668;

Utility model application

1. **Cristea Mario**, Matache Mihai-Gabriel, (INMA București) Zapciu A. (INCDMTM), Tudor E. (INCDIE ICPE) Carpus E. (INCDTP), Laslo L. (INCDPM), 2019, *Technologies for carrying out agricultural works using ecological machines: electric tractor prototype*, nr. request M 164343;

Selective Bibliography

- [1] MADR, „DATE GENERALE DESPRE AGRICULTURA ROMÂNIEI,” 2015. [Interactiv]. Available: <https://www.madr.ro/docs/agricultura/agricultura-romaniei-2015.pdf>.
- [2] Parlamentul European, „Jurnalul Oficial al Uniunii Europene 2.3.2013 L60/I,” 02 mar 2013. [Interactiv]. Available: http://publications.europa.eu/resource/cellar/79ce6e68-96dc-418f-b104-a0c0b7130cee.0006.03/DOC_1.
- [3] I. Conf.univ.dr.ing. BĂISAN, „TRACTOARE, AUTOMOBILE ȘI SISTEME DE PROPULSIE A MAȘINILOR AGRICOLE - partea I,” 2020. [Interactiv]. Available: <https://mec.tuiasi.ro/wp-content/uploads/2020/11/TASPMA-curs-partea-I-a.pdf>.
- [4] A. Zhuravlev, D. Sychev și N. Savosteenko, „Mass-dimensional parameters of traction drive,” *Procedia Engineering*, pp. 946-950, 2015.
- [5] A. Ioniță, „Răsărire uniformă cu semănătoarea John Deere,” 15 oct 2022. [Interactiv]. Available: <https://www.agrimedia.ro/articole/rasarire-uniforma-cu-semanatoarea-jd>.
- [6] FENDT, „Fendt FutureFarm,” 05 mar 2022. [Interactiv]. Available: <https://www.fendt.com/int/e100-vario>.
- [7] V. Măț, „AGRICULTURA cu MAȘINI INTELIGENTE (II),” *Revista Ferma*, p. 1, 02 Noembrie 2017.
- [14] S. Sinha, „Revolution in Agriculture Technology: Best Electric Tractors for Farmers,” 24 noi 2021. [Interactiv]. Available: <https://tractornews.in/articles/revolution-in-agriculture-technology-best-electric-tractors-for-farmers>.
- [19] L. Drotleff, „greenhousegrower,” 06 mai 2021. [Interactiv]. Available: <https://www.greenhousegrower.com/technology/why-horticulture-is-ripe-for-artificial-intelligence/>.
- [20] IBEX Automation LTD, „IBEX,” 13 iun 2018. [Interactiv]. Available: <http://www.ibexautomation.co.uk/>.
- [21] E. Black și L. Kolodny, „This robot can pick tomatoes without bruising them and detect ripeness better than humans,” 11 mai 2019. [Interactiv]. Available: <https://www.cnn.com/2019/05/11/root-ai-unveils-its-tomato-picking-robot-virgo.html>.
- [22] S. Crowe, „Abundant Robotics shuts down fruit harvesting business,” 6 iul 2021. [Interactiv]. Available: <https://www.therobotreport.com/abundant-robotics-shuts-down-fruit-harvesting-business/>.
- [23] B. Heater, „Abundant’s apple harvesting robots get their first commercial deployment,” 26 mar 2019. [Interactiv]. Available: <https://techcrunch.com/2019/03/25/abundants-apple-harvesting-robots-get-their-first-commercial-deployment/>.
- [24] iso-group, „Roboplant,” 05 noi 2022. [Interactiv]. Available: <https://www.iso-group.nl/en/machines/roboplant>.
- [25] ENERGID, „energid.com,” 19 sep 2021. [Interactiv]. Available: <https://www.energid.com/industries/agricultural-robotics>.
- [26] Agrobot, „www.agrobot.com,” 10 ian 2023. [Interactiv]. Available: <https://www.agrobot.com/e-series>.
- [27] Metomotion, „Greenhouse Robotic Worker,” 05 noi 2022. [Interactiv]. Available: <https://metomotion.com/robotic-worker/>.
- [28] Harvest Automation, „MOBILE ROBOTS FOR INDUSTRIAL PRODUCTIVITY,” 09 mar 2022. [Interactiv]. Available: <https://www.public.harvestai.com/>.
- [32] B.-A. Mordechai și M. Francesco, *Elements of Robotics*, Springer Cham, 2018.
- [33] J. J. Istvan, „Gyomirtás automatikusán, minimális herbiciddel - Bemutakozik az ecoRobotix pont-permetező robot,” *Agroforum Online*, p. 1, 26 oct 2018.
- [34] C. Bo-Chiuan, G. Jen-Chiun și L. Jhih-Hong, „Adaptive power management control of range extended,” *The 6th International Conference on Applied Energy – ICAE2014*, pp. 67-70, 2014.
- [35] I. D. Păunescu și M. Constantin, *Tractoare și Automobile, mecanica sistemelor de propulsie*, București: Universitatea Politehnica București, 1993.
- [36] Ș. Tabacu, I. Tabacu, T. Macarie și E. Neagu, *DINAMICA AUTOVEHICULELOR, Îndrumar de proiectare*, Pitești: Universității din Pitești, 2004.
- [37] I. Băisan, *TRACTOARE, AUTOMOBILE ȘI SISTEME DE PROPULSIE A MAȘINILOR AGRICOLE*, Iași, 2020.
- [38] N. T. Macarie, I. Vieru și H. Bădărău-Șuter, *TRANSMISII AUTOMATE, AUTOMATIZATE ȘI CONTINUE PENTRU AUTOMOBILE*, Iași: PIM, 2018.
- [39] I. D. Păunescu, *Tractoare și automobile*, București: U.P.B., 1993.
- [40] Y. Kazakov, V. Batmanov și V. Medvedev, „Wheel drive with integrated differential,” *IOP Conference Series: Earth and Environmental Science*, 2021.
- [46] M. Cristea, L. Vlăduțoiu, I. A. Grigore și R. D. Cristea, „TYPES OF ELECTRIC MOTOR CONTROLLERS THAT CAN BE USED ON AGRICULTURAL ELECTRIC TRACTORS,” *Analele Universității din Craiova*,

- seria Agricultură –Montanologie –Cadastru (Annals of the University of Craiova -Agriculture, Montanology, Cadastre Series), pp. 235-250, 2021.*
- [47] Kellycontrollers, „KellyKAC-8080NUserManualV1.13-120N-3.pdf,” 18 feb 2023. [Interactiv]. Available: <https://media.kellycontroller.com/new/KellyKAC-8080NUserManualV1.13-120N-3.pdf>.
- [48] Kellycontrollers, „kls7245h,” 18 mai 2022. [Interactiv]. Available: <https://www.kellycontrollers.eu/kls7245h>.
- [49] CurtisInstruments, „1239E_datasheet_en.pdf,” 20 iul 2021. [Interactiv]. Available: https://cdn.curtisinstruments.com/products/datasheets/1239E_datasheet_en.pdf.
- [50] EvolveElectrics, „1239-e,” 09 apr 2020. [Interactiv]. Available: <https://evolveelectrics.com/products/1239-e>.
- [64] M. Cristea, M. G. Matache, C. Sorică, I. A. Grigore, I. Grigore, E. Sorică, I. Dumitru, R. D. Cristea și F. Nenciu, „STUDY REGARDING THE NOISE LEVEL GENERATED BY AN ELECTRIC POWERED AGRICULTURAL VEHICLE,” *ISB INMA TEH*, pp. 734-738, 2020.
- [65] Curtis, „Handheld Programmer Model 1313,” 21 dec 2019. [Interactiv]. Available: https://cdn.curtisinstruments.com/products/datasheets/1313_datasheet_en.pdf.
- [66] HMS_Industrial_Networks_AB, „USB-to-CAN FD,” 09 dec 2019. [Interactiv]. Available: <https://www.ixxat.com/technical-support/pages/can-interfaces?ordercode=1.01.0351.12001>.
- [67] EVEA, „SEVCON Clearview configurable CANopen colour display,” 31 mar 2023. [Interactiv]. Available: <https://evea-kartmasters.fr/en/controller-programming-tools/1640-sevcon-clearview-configurable-canopen-colour-display.html>.
- [68] Electric_Drive_Engineering_Pty_Ltd, „SEVCON Clearview Display,” 04 feb 2020. [Interactiv]. Available: <https://electricdriveengineering.com.au/product/sevcon-clearview/>.
- [69] Curtis, „Windows PC Software Tool for Curtis Programmable Devices Model 1314,” 11 dec 2019. [Interactiv]. Available: https://cdn.curtisinstruments.com/products/datasheets/1314_datasheet_en.pdf.
- [79] HBM, „Strain gauge amplifier – QuantumX MX1615B / MX1616B,” 6 feb 2020. [Interactiv]. Available: https://www.hbm.com/en/3053/quantumx-mx1615b-bridge-amplifier-for-strain-gauges/?product_type_no=QuantumX%20MX1615B/MX1616B%20Strain%20Gauge%20Amplifier.
- [80] HBM, „Strain gauge amplifier – QuantumX MX1615B / MX1616B,” 25 apr 2021. [Interactiv]. Available: https://www.hbm.com/en/3053/quantumx-mx1615b-bridge-amplifier-for-strain-gauges/?product_type_no=QuantumX%20MX1615B/MX1616B%20Strain%20Gauge%20Amplifier.
- [81] M. Cristea, M. G. Matache, I. G. Grigore, L. Vlăduțoiu, C. Persu și I. Dumitru, „STUDY ON THE USE OF AUTOMOTIVE BATTERY PACK FOR DRIVING AGRICULTURAL VEHICLES,” *ISB INMA TEH*, pp. 106-115, 2019.
- [82] I. Arinata, A. Ahmad Husman, W. Dito, H. Hilwadi și A. Purwadi, „An easy speed measurement for incremental rotary encoder using multi stage moving average method,” *International Conference on Electrical Engineering and Computer Science (ICEECS)*, 2015.
- [83] M. G. Matache, M. Cristea, I. Găgeanu, A. Zapciu, E. Tudor, E. Carpus și L. D. Popa, „SMALL POWER ELECTRIC TRACTOR PERFORMANCE DURING PLOUGHING WORKS,” în *International Symposium ISB-INMA TEH 2020*, București, 2020.
- [84] CDEP, „Consumuri specifice de motorină pentru lucrări mecanizare,” 4 aug 2020. [Interactiv]. Available: <https://www.cdep.ro/proiecte/2006/600/20/6/ax2.pdf>.
- [85] M. Ehsani, Y. Gao, S. E. Gay și A. Emadi, *Modern Electric, Hybrid Electric, and Fuel Cell Vehicles Fundamentals, Theory, and Design*, Washington, D.C: CRC PRESS, 2005.
- [86] M. Cristea, M. G. Matache, C. M. Sorica, S. Ș. Biriș, N. Ungureanu și R. D. Cristea, „STUDY ON THE BEHAVIOR OF A BATTERY MOUNTED ON AN ELECTRIC TRACTOR PROTOTYPE,” *INMATEH Agricultural Engineering*, 2020.
- [87] M. Z. Frank și D. G. Robert, *Traction and Tractor*, Louisville, Kentucky, USA: American Society of Agricultural Engineers, 2003.
- [88] Maurelma, „LiFePO4/3_3KW_User_Manual_mau.pdf,” 17 noe 2019. [Interactiv]. Available: https://www.maurelma.ch/Produkte/Ladegeraete/LiFePO4/3_3KW_User_Manual_mau.pdf.
- [89] Agri_Expert, „Moteur complet tracteur AVTO Belarus MTZ 80,MTZ 82,MTZ 900,MTZ 920 sans démarreur,” 9 iun 2020. [Interactiv]. Available: <https://www.agri-expert.fr/moteur-complet-sans-demarreur-pour-avto-belarus-mtz80-mtz82-mtz900-mtz920.html>.
- [90] „SEVCON Clearview configurable CANopen colour display,” 31 mar 2023. [Interactiv]. Available: <https://evea-kartmasters.fr/en/controller-programming-tools/1640-sevcon-clearview-configurable-canopen-colour-display.html>.
- [91] F. M. Zoz și R. D. Grisso, *Traction and Tractor Performance*, Louisville, Kentucky, USA: American Society of Agricultural Engineers, 2003.

Annexes

Abbreviations

BMS	Battery Management System
CAN	Controller Area Network
CAN FD	Controller Area Network Flexible Data-Rate
CIT	Curtis Integrated Toolkit
GLONASS	GLObal'naia NAVigaționaia Sputnikovaia Sistema
GNSS	Global Navigation Satellite System
GPS	Global Positioning System
HBM	Hottinger Baldwin Messtechnik
KMC	Kelly Motor Controllers
LCD	Liquid Crystal Display
INMA	National Research-Development Institute for Machines and Installations for Agriculture and the Food Industry
m.a.c.	compression ignition engine
m.a.s.	engine with spark ignition
.NET	proprietary software developed by Microsoft
RMS	Root mean square
SoC	State of charge
TACT	Test, analysis and calibration tool
TE.	Electric tractor
USB	Universal Serial Bus
VCL	Software package dedicated to controllers from Curtis

List of notations

α	is the angle of inclination of the running surface [rad/s];
α_c	is the descent angle [degrees];
α_u	is the angle of the climb slope [degrees];
$\alpha_{max u}$	is the maximum climb angle [degrees];
$\alpha_{max c}$	is the maximum descent angle [degrees];
α_v	is the angle of maximum transverse stability [degrees];
ϵ	is the slip coefficient;
σ	is the tension between the contact surface of the wheel and the ground;
Δ_t	is the time required for rotation [s];
δ	is slip coefficient;
λ	is the longitudinal stability coefficient;
λ_{lim}	is the maximum limit of the stability coefficient;
$\Phi_{ad'}$ și $\Phi_{ad''}$	are wheel weight utilization coefficients;
φ_a	is adhesion coefficient;
φ_{ga}	is coefficient of use of weight on the wheel;
φ_m	is the effective adhesion coefficient;
φ_a	is the coefficient of effective use of adhesion;
φ_m	is the adhesion utilization coefficient;
ω	is the angular velocity of the motor [rad/s];
ω	is the angular velocity vector of the wheel [rad/s];
ω_g	is the angular velocity of the motor shaft [rad/s];
ω_i	is wheel angular velocity [rad/s];
ω_m	is the maximum engine speed [rad/s];
ω_n	is the nominal engine speed [rad/s];
ω_M	is the maximum engine speed [rad/s];
ω_p	is the speed caused by the slip of the electromagnetic field [rad/s];
ρ	is air density, 1.225 at sea level, 15 degrees Celsius [kg / m ³];
μ_p	is the tire friction coefficient on the rolling surface;
η	is the total yield [%];
η_{card}	is cardan yield [%];
η_{cv}	is the gearbox efficiency [%];
η_s	is slip yield [%];
η_f	is running efficiency [%];
η_m	is the engine efficiency [%];
η_{tc}	is the central transmission efficiency [%];
η_{tmc}	is the efficiency of the mechanical torque transformer [%];
η_{tf}	is the final transmission efficiency [%];
η_{tr}	is the total yield [%];
τ	is the tangential stress [N];
a	is the distance from the center of gravity to the front axle [m];

a'	is the new value of the distance between the front axle and the center of gravity, when the battery is moved to the rear [m];
a''	is the new value of the distance between the front axle and the center of gravity, when the battery is moved to the rear [m];
a_{ab}, b_b, c_c	are coefficients that depend on the tire, pressure and running surface;
A	is the area of the contact surface between the wheel and the ground [m ²];
A_c	is the total area of the tire contact surface;
A_f	is the front surface of the tractor [m ²];
a_m	is the displacement in the direction of movement of the surface normal [m];
a_i	is the distance from the center of gravity to the respective equipment [m];
A_t	is tractor acceleration [m/s ²];
b	is the distance from the center of gravity to the rear axle [m];
b'	is the new value of the distance between the rear axle and the center of gravity, when the battery is moved to the front [m];
b''	is the new value of the distance between the rear axle and the center of gravity, when the battery is moved to the front [m];
b_p	is the tire width [m];
B	is the gauge [m];
c	is elasticity coefficient;
C	is a coefficient that depends on the deformation of the running surface;
C_{bat}	battery capacity [Ah];
C_d	is aerodynamic coefficient;
C_g	is the position of the center of gravity of the tractor [m];
C_{inc}	charging current [A];
C_{rr}	is the rolling resistance coefficient of the wheels;
D	is the dynamic factor;
D_{cr}	is the deformation of the running path [m ²];
E	is the energy [J];
E_b	is the energy that reaches the battery [kWh];
E_{out}	is the energy consumed from the battery [Ah];
f_m și f_d	are the rolling resistance coefficients;
f_t	is the driving force [N];
f_i	is the inertia force [N];
f_{tr}	is the tangential reaction on the bridges [N];
f_g	is the operating weight [N];
f_n	is the normal force of the tractor [N];
f_w	is air resistance [N];
f_c	is the rolling resistance coefficient of the driven wheel;
F_α	is the force used to climb the inclined plane [N];
F_a	is the air resistance [N];
F_c	is the traction force [N];
F_j	is the force required to accelerate the tractor [N];
F_f	is the force required to overcome the friction forces [N];
F_r	is the rolling resistance force [N];
F_t	is the reaction parallel to the chassis plane [N];
F_m	is the driving force [N];
F_m'	is the driving force when climbing the slope [N];
F_s	is the reaction parallel to the chassis plane [N];
f_m	is rolling resistance coefficient;
F_m	is the average traction force;
g	is the gravitational acceleration [m/s ²];
G	is the weight of the tractor [N];
G_a	is the total weight [N];
G_{ad}	is the weight on the wheel [N];
G_j	is the additional weight (ballast), in front of the tractor [N];
G_f	is the weight on the front axle [N];
G_m	is maximum weight [N];
G_s	is the weight on the rear axle [N];
G_t	is the operating weight [N];
h_i	is the height of the subassembly from the ground [m];
h_m	is the height of the machine weight center [m];
h_g	is the height of the center of gravity [m];
h_l	is height center weight ballast [m];
h_p	difference between dynamic radius and wheel radius [m];
i, j și k	are the directions of the axes Ox, Oy and Oz ;
i_{cv}	is the gearbox ratio;
i_t	is the total transmission ratio;
i_{tc}	is the central transmission ratio;
i_{tmc}	is the ratio of the mechanical torque transformer;
i_{tf}	is the final transmission ratio;
i_{tr}	is the total transmission ratio;
j	is the deformation of the terrain in the tangential plane;
J_c	is the moment of inertia of the driven wheel relative to the axis of rotation [Nm];
J_m/J_{ms}	are the moments of inertia of the moving elements of the wheels [Nm];
J_d	is the moment of inertia of the wheel relative to the axis of rotation at the drive wheel [Nm];

J_{mm}	is the moment of inertia of the motor [Nm];
J_m	is the moment of inertia of the wheel with reference to the wheel axis [Nm];
K	is adaptability coefficient;
k	is the ground deformation [m];
k_y	is the maximum strain [m];
k_0	is the minimum deformation [m];
k_r	is the wheel radii mismatch coefficient;
k_{cin}	is kinematic mismatch coefficient;
L	is wheelbase [m];
I_1	is current intensity through coil 1 of the motor [A];
L_m	is the inductance of the coil [H];
I_m	is the current at the motor coil terminals [A];
M	is the motor torque [Nm];
m	is the total mass [Kg];
m_0	is own mass [kg];
m_a	is the front axle mass [kg];
M_a	is the engine torque [Nm];
m_c	is the mass of the driven wheel [kg];
M_e	is the effective moment [Nm];
M_e'	is the effective moment when climbing the slope [Nm];
m_f	is the front axle mass [N];
M_{fd}	is the moment of resistance at the drive/steer wheel axle [Nm];
M_{fc}	is the friction moment in the wheel bearings [Nm];
M_{fm}	is the moment of the friction force in the wheel bearings [Nm];
M_g	is the moment at the shaft of the electric motor [Nm];
m_i	is the mass of the equipment [kg];
m_m	is the mass of the wheel [kg];
M_{mr}	is the wheel moment (radial) [Nm];
M_{max}	is the maximum engine moment [Nm];
M_n	is the moment at actual speed [Nm];
M_m	is the motor torque [Nm];
M_m'	is the moment of the motor when climbing the slope [Nm];
m_s	is the mass on the rear axle [Kg];
m_u	is the payload [kg];
n	is the speed [rpm];
n_g	is the maximum idle speed [rpm];
η_G	is the ratio of tractor mass to payload;
η_m	is the engine efficiency [%];
n_m	is the engine speed [rpm];
n_{min}	is the minimum speed [rpm];
n_n	is the rated engine speed [rpm];
N_n	is the read engine speed [rpm];
n_M	is the speed at the maximum moment [rpm];
P_{b-in}	is the power reaching the battery from the motor/generator [Ah];
P_{b-out}	is the power from the battery reaching the motor [Ah];
P_g	is the power of the motor at the axis [W];
P_m	is the motor power [W];
$P_{def.terent}$	is the power required for ground deformation [W];
$P_{hist.pneu}$	is the power lost by hysteresis to tire deformation [W];
P_e	is the power at the wheel [W];
r	is the position vector from the center of the wheel to some point N [m];
R	is the reaction produced by a towed machine [N];
R_1	is the resistance of motor coil 1 [Ω];
r_d	is the radius of the deformed wheel [m];
r_m	is the dynamic radius of the wheel [m];
r_o	is the wheel radius [m];
Q_c	is the vertical load of the chassis and wheel weight on horizontal terrain [N];
Q_{r1} și Q_{r2}	is the product of the compressive stress and the total area of the front wheel's ground contact surface [N];
Q_{s1} și Q_{s2}	is the product of the compressive stress and the total area of the ground contact surface of the rear wheel [N].
Q_m	is the vertical loading of the chassis and wheel weight on inclined terrain [N];
Q'_m	is the increased wheel weight [N];
Q''_m	is the increased wheel weight [N];
Q_{mm}	is the average weight per driven wheel;
t	is the pitch of the adhesion edges;
T_{inc}	is charging time [s];
T_r	is the actual traction (wheel force) [N];
U	is the voltage [V];
U_n	is the nominal voltage [V];
\vec{V}	is the displacement velocity vector [m/s];
\vec{V}_{-r}	is the velocity vector of the wheel center [m/s];
v	is the travel speed [m/s];
V	is the voltage [V];
v_{al}	is the sliding speed [m/s];
v_{pat}	is the skating speed [m/s];

v_r	is the actual speed [m/s];
v_t	is theoretical speed [m/s];
v_w	is wind speed [m/s];
x și z	are the coordinates of some point, M ;
X_c	is the tangential component of the ground reaction on the wheel [N];
$X_{def.teren}$	is the horizontal component of the ground response to deformation [N];
X_m și X_d	are the tangential reactions on the axles [N];
$X_{m s}$	is the tangential reaction at the rear wheels [N];
$X_{m f}$	is the tangential reaction at the front wheels [N];
X_{mb}	is the reactance of the coil [Ω];
Y'	is the soil reaction at wheel 1 [N];
Y''	is the ground reaction at wheel 2 [N];
Z'	is the normal soil reactions on wheel 1 [N];
Z''	is the normal ground reactions on wheel 2 [N];
Z_c	is the ground reaction on the wheel [N];
Z_d	is the weight on the front axle [N];
$Z_{d nec}$	is weight [N];
Z_m și Z_d	are the normal soil reactions on the decks [N];